TOPICAL REVIEW

Plasma for cancer treatment

To cite this article: Michael Keidar 2015 *Plasma Sources Sci. Technol.* **24** 033001

IOP Publishing Plasma Sources Science and Technology

Plasma Sources Sci. Technol. **24** (2015) 033001 (20pp) doi:10.1088/0963-0252/24/3/033001

Topical Review

Plasma for cancer treatment

Michael Keidar[1,2]

[1] Department of Mechanical and Aerospace Engineering, The George Washington University, Washington DC 20052 USA
[2] Department of Neurological Surgery, The George Washington University, Washington DC 20052 USA

E-mail: keidar@gwu.edu

Received 11 December 2014, revised 9 March 2015
Accepted for publication 7 April 2015
Published 20 May 2015

Abstract

Plasma medicine is a relatively new field that grew from research in application of low-temperature (or cold) atmospheric plasmas in bioengineering. One of the most promising applications of cold atmospheric plasma (CAP) is cancer therapy. Convincing evidence of CAP selectivity towards the cancer cells has been accumulated. This review summarizes the state of the art of this emerging field, presenting various aspects of CAP application in cancer such as the role of reactive species (reactive oxygen and nitrogen), cell cycle modification, *in vivo* application, CAP interaction with cancer cells in conjunction with nanoparticles, and computational oncology applied to CAP.

Keywords: cold atmospheric plasma, cancer therapy, plasma selectivity

(Some figures may appear in colour only in the online journal)

1. Introduction

Plasma medicine is a relatively new scientific field that grew from research in application of a low-temperature (or cold) atmospheric plasmas in bioengineering [1–3]. It became apparent that cold atmospheric plasma (CAP) interaction with tissue allows targeted cell removal without necrosis, i.e. cell disruption [4]. In fact, it was determined that CAP affects cells via a programmable process called apoptosis [1–4]. Apoptosis is a multi-step process leading to cell death and this process is the one inherent to cells in the human body.

It should be pointed out that electrical discharges in air were used for therapeutic applications from as early as the beginning of the 20th century [5] and the first plasma coagulator was introduced by Morrison [6] in 1977. Georges Lakhovsky and Arsene D'Arsonval invented the so-called multiple-wave oscillator that was proposed to use in cancer treatment [7]. Recall that the majority of earlier applications of plasmas in medicine were primarily based on the thermal effects of plasma [8]. A good example of utilization of the plasma thermal effect is the argon plasma coagulation (APC) that is employed for tissue cut and coagulation [9, 10]. Most applications of plasmas in medicine nowadays are associated with more gentle non-thermal effects.

CAP contains a variety of charged particles, reactive oxygen species (ROS), reactive nitrogen species (RNS), UV etc. It is known that both ROS and RNS can promote oxidative stress and trigger different signaling pathways in cells. The mechanism of CAP interaction with living tissue remains elusive. Different authors have explored the roles of various species and there is no consensus about the primary mechanism. Recall that the plasma species are highly selective in interacting with living tissue and can have either 'plasma killing' (such as O) or 'plasma healing' (such as NO) effects [11].

CAP is already proven to be effective in wound healing, skin diseases, hospital hygiene, sterilization, antifungal treatments, dental care and cosmetics targeted cell/tissue removal [12–18]. More recently, the potential of CAP application in cancer therapy was explored [19–22]. It was demonstrated that the CAP treatment leads to selective eradication of cancer cells *in vitro* and reduction of tumor size *in vivo* [23–27]. ROS metabolism and oxidative stress responsive gene deregulation have been detected [21, 22]. In general, the number of publications related to CAP application in cancer has increased exponentially over the last few years as indicated in figure 1. As such, an overall analysis of the field in view of recent publications might benefit the community working on plasma

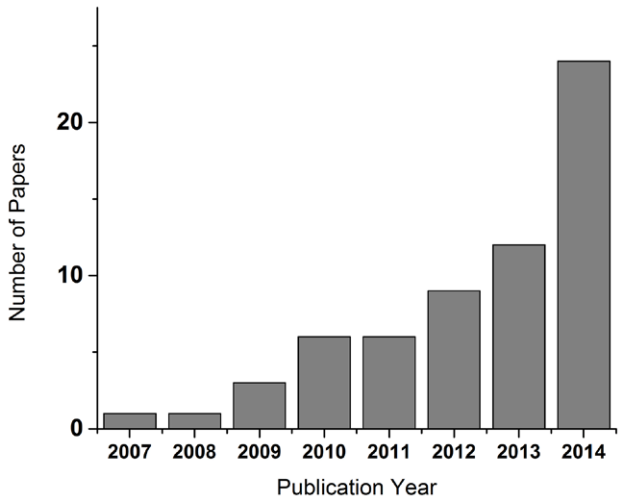

Figure 1. Number of publication on plasma application in cancer. (Courtesy of Dayun Yan).

applications and general journal readership. This Topical Review is devoted to a description of the state of the art of CAP application in cancer.

2. Cold atmospheric plasmas: measurements and simulations

2.1. CAP sources

Sources producing CAP can be broadly classified into three major groups chiefly by the way biological objects are treated. This includes direct, indirect and hybrid approaches. Typical images of plasma devices are shown in figure 2.

In a *direct* CAP source living tissue serves as one of the electrodes becoming in active part of the discharge. A typical example of a direct plasma source is the dielectric barrier discharge (DBD) [3]. In this arrangement a fraction of the current flows through the living tissue in the form of a small conduction current. The current is typically limited to minimize the thermal effects and electrical stimulation of the muscles.

In an *indirect* CAP source the active plasma species are transported by a gas flow from the main discharge arc. Various plasma jets are typical examples of this approach [1–4].

In the *hybrid* configuration plasma generation of the direct CAP source is combined with that of the indirect CAP source by creating a current-free condition in the tissue. This condition is ensured by placing a grounded mesh electrode having resistance smaller than that of the skin [28, 29].

It should be pointed out that the results presented in this review are generally dependent on the type of plasma used. Thus it is important to pay attention to the details of the particular plasma source used in each experiment.

2.2. Brief description of plasma diagnostics

Various diagnostic tools have been developed to probe CAP. Nowadays routine diagnostics include intensified charge-coupled device (ICCD) cameras, optical emission spectroscopy and electrical measurements of the discharge properties [30–35]. Time-resolved measurements of the emission were performed for the case of very dense plasmas ~10^{16}–10^{17}cm^{-3} using passive optical emission spectroscopy [36]. In these experiments gas rotational temperature (which is based on a fit of measured results with simulations) and electron density (which is based on Stark broadening) were determined. Three different modes of operation, namely chaotic, bullet and continuous, were proposed based on the experimental data [37, 38]. Various active spectroscopic techniques were utilized in recent works, namely laser-induced fluorescence spectroscopy, diode laser absorption spectroscopy and Rayleigh, Thomson and Raman scattering of laser radiation on microplasmas [39–46]. These measurements uncovered spatially resolved distribution (down to 10–50 m) of densities and temperatures of various plasma species such as electrons, molecules and metastable atoms. Recently, new methods including scattering of microwave radiation (RMS) on the plasma channel and streamer control by means of external electric potential were proposed allowing temporally-resolved measurements of plasma density and conductivity, electrical currents in plasma jets, electric potential and charge carried in the front of ionization [47–53].

An example showing the time-resolved evolution of discharge electrical and plasma parameters as well as ICCD camera images for typical 20–30 kHz CAP jet is shown in figure 3. One can see that the breakdown occurs once per period of the ac high voltage during a positive half wave at the central electrode. The breakdown of the interelectrode gap is indicated by the peak of the discharge current (I_d). The discharge current increases to about 6–8 mA at about 1 μs after the breakdown and then decays with characteristic times of about 3 μs. This stage of the discharge is characterized by its presence in the interelectrode gap only with no ionization wave outside the discharge tube. The next stage of the discharge starts at about 3 μs after the breakdown when the ionization front (streamer) propagates out of the discharge tube into the open air. The streamer propagates axially about 4–5 cm with a speed of about 2×10^6 cm s^{-1} along the helium flow until it decays at $t \approx 5\,\mu$s as can be seen from a series of instant photographs. Measurements of plasma density in the streamer channel conducted using RMS yield an averaged value of the electron density along the streamer channel of about 3–4 $\times$ 10^{12} cm^{-3}. Recall that the plasma ionization degree in the jet is very low ~10^{-6}–10^{-7} (gas density at 1 atmosphere and 300 K is around 2×10^{19} cm^{-3}). Electrical potential of the streamer tip (U_h) measured during streamer development is indicated as well. It can be seen that the streamer tip carries a potential close to that of the central electrode. CAP parameters measured by various diagnostics are gathered in table 1.

Various optic-based techniques were employed for atmospheric plasma diagnostics. A general review of the optical diagnostic methods and approaches applied to study the atmospheric plasmas and, in particular, fundamentals of streamer discharges was presented by Simek [54].

The generation of radicals by CAP was studied by various groups. In one study the hydroxyl OH radical density inside the biosolutions was investigated experimentally by

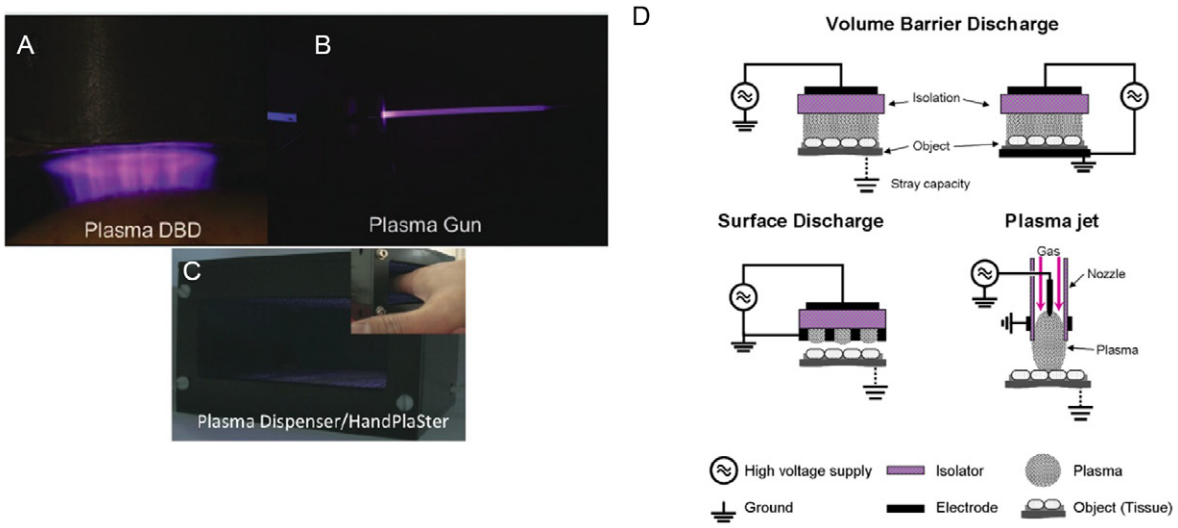

Figure 2. Image of typical cold atmospheric plasma. (A) DBD plasma source; (B) cold atmospheric plasma jet; (C) hybrid plasma device. (D) After Weltmann *et al* [29], CAP sources for therapeutic applications. Published with permission from *Int. J. Cancer* [22], IOP [28] and IUPAC [29].

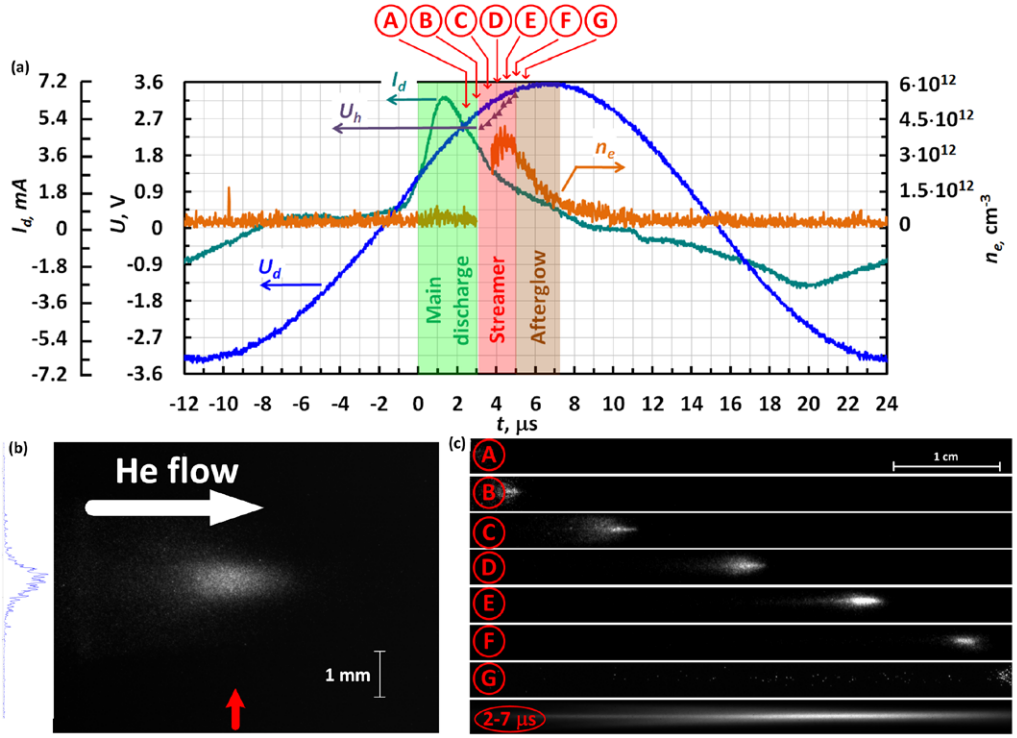

Figure 3. (a) Temporal evolution of discharge current, voltage and plasma density in the streamer. Three stages of the streamer development, namely main discharge in the interelectrode gap (green bar), streamer growth (red bar) and afterglow of the streamer channel (blue bar) are shown. (b) Series of instant photographs demonstrating the streamer growth (100 ns exposure time). The photographs were taken at the moments of time indicated by the letters A–G. The last image in the series was taken with, exposure time of 5 μs covering temporal interval 2–7 μs. (c) Typical high-magnification of the streamer tip. The diagram on the left shows distribution of the intensity along the direction indicated by the red arrow. A diameter of the streamer channel equal to 0.6 mm was utilized throughout the paper. Courtesy of A Shashurin and M Keidar 2015 *Phys. Plasmas*, in press

Table 1. Parameters of the streamer on the growth stage (He flow = 5–10 L min^{-1}, U_{HV} = 2.5–4 kV, 20–30 kHz frequency, [51].

Head charge, electrons	Streamer length, cm	Speed of ionization front, cm s^{-1}	Streamer radius, cm	Characteristic electrical field in head vicinity, V cm^{-1}	Average plasma density in the streamer, cm^{-3}
1–2 × 10^8	4–5	2 × 10^6	3 × 10^{-2}	about 10^4–10^5	3–4 × 10^{12}

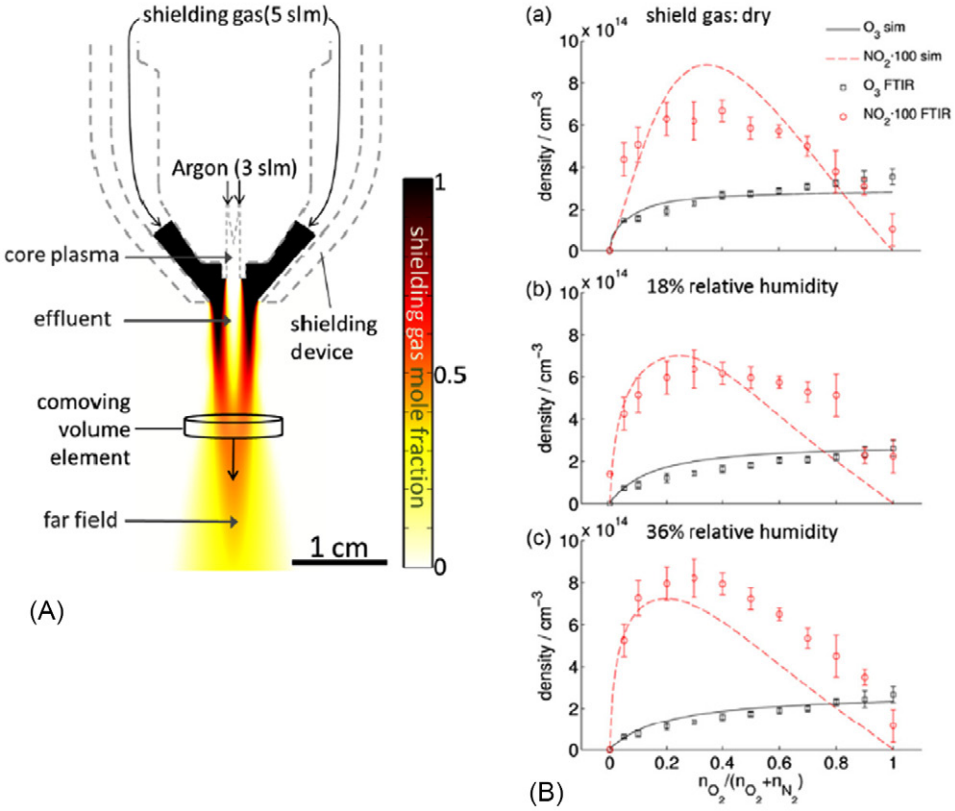

Figure 4. (A) Sketch of the kinpen 09 geometry and visualization of the shielding gas curtain by CFD simulation. (B) Density of ozone and nitrogen dioxide upon oxygen to nitrogen shielding gas variation (a)–(c) at different humidity levels and humidity variation at O_2/N_2 = 20/80. Published with permission from IOP [56].

ultraviolet absorption spectroscopy [55]. The densities of the OH radical species inside the deionized water, Dulbecco's modified eagle medium (DMEM), and phosphate buffered saline are measured to be about 1–2 × 10^{16}cm^{-3}. It was also pointed out that the critical hydroxyl OH radical density for the lung cancer H460 cells to cause an apoptosis is observed to be around 0.3 × 10^{16} cm^{-3} if 60 s plasma treatment is used.

The effect of the gas composition on the reactive species generation was investigated using the combination of Fourier transform infrared (FTIR) spectroscopy, computational fluid dynamics (CFD) simulations and zero dimensional kinetic modeling of the gas phase chemistry [56]. In this work, an argon CAP device driven at a frequency of 1.1 MHz was used as shown schematically in figure 4(A). The ozone production in the plasma jet continuously increases with the oxygen content, while it significantly drops with humidity increase. On the other hand, the production of nitrogen dioxide reaches its maximum with about 30% oxygen content in the case of shield gas (dry) as shown in figure 4(B).

Nitric oxide (NO) is one of the important chemically active species playing a vital role in medicine. Generation of NO by CAP was studied by several groups [57, 58]. Absorption spectroscopy and optical emission spectroscopy was used by Pipa *et al* [58] to measure the NO production rate in an atmospheric pressure plasma jet. Recently laser-induced fluorescence (LIF), OES and molecular beam mass spectrometry (MBMS) were employed to measure the absolute density of NO in an atmospheric plasma jet [59]. Representative results of NO measurements [57, 59] are shown in figure 5. NO density is shown (figure 5(a)) at different values of the power dissipated in the plasma. One can see that the NO density is proportional to the average power dissipated in the plasma. LIF and MBMS measurements of NO are compared in figure 5(b). It can be seen that the NO density decreases with increasing distance in the effluent. It was suggested [57] that it is the result of outwards diffusion and reactions of NO with O_3. In another study [58] it was shown that the NO density initially increases with power saturating at about 30 W. It should be pointed out that the maximum NO density increases approximately linearly with the premixed air concentration [58]. It was argued [58] that at higher air concentration the plasma size decreases, and it becomes more difficult to sustain the discharge.

2.3. CAP modeling and simulations

One of the first models of a streamer was proposed by Dawson and Winn [60] in which the streamer head was considered as autonomous and insulated from electrodes. In later works the streamer channel was described as a perfectly conducting ellipsoid [61]. Various approaches to streamer modeling are outlined in a recent review [62]. While analytical solutions developed over several decades are very useful, a more involved and detailed understanding is possible via numerical simulations.

Numerical simulations of streamers in helium–air mixture were conducted [63, 64]. Values of streamer propagation velocities (10^6–10^7 cm s^{-1}), electrical field in the streamer head

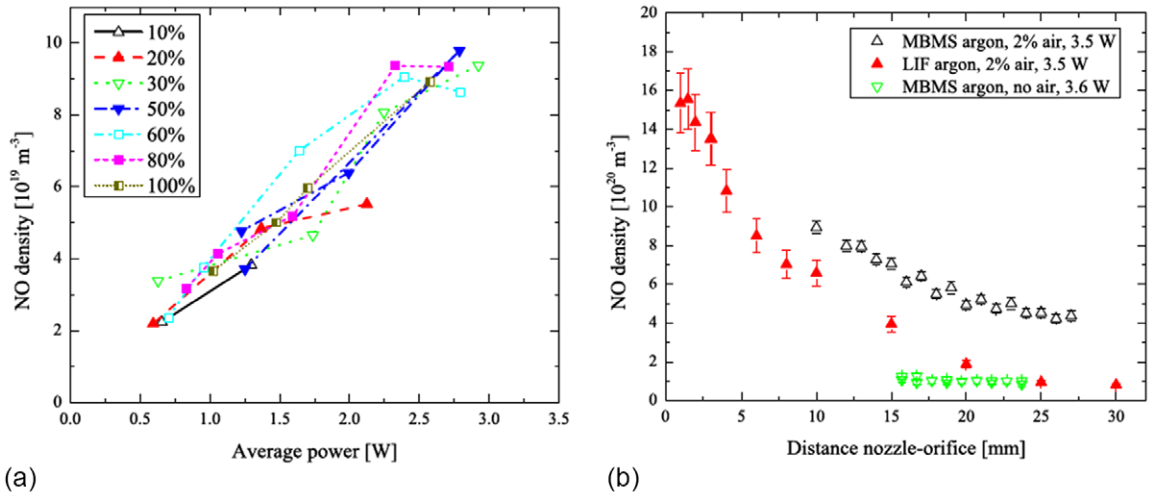

Figure 5. (a) NO density as a function of the average power at different duty cycles. (b) Comparison of the NO density measured by LIF and MBMS, as a function of distance between the nozzle of the jet and the metal orifice. Published with permission from IOP [57].

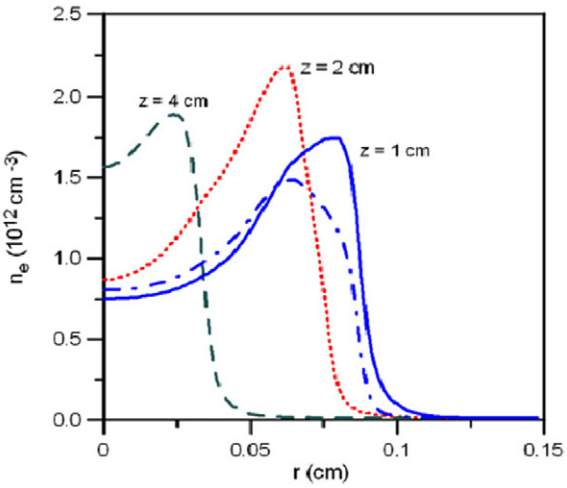

Figure 6. Calculated radial distributions of number densities of electrons at various axial positions, for time moments 50 ns ($z = 1$ cm), 130 ns ($z = 2$ cm) and 430 ns ($z = 4$ cm). Dotted–dashed lines show the results for $z = 1$ cm obtained without account of Penning reactions. Published with permission from IOP [63].

vicinity (~10 kV cm^{-1}), and plasma density in the streamer channel (10^{12}–10^{13}cm^{-3}) were predicted in these simulations. While several authors utilized an assumption about the leading role of the Penning process in plasma bullet dynamics, calculations performed in [63, 64] raised some questions about that assumption. One can see (figure 6) that the Penning process does not have a significant effect on electron density. Patterns of streamer structure in both cases, with and without account of this reaction, are nearly the same as suggested in [63, 64]. It was also predicted that two types of cross-sectional shapes of streamer channel can be formed, namely with plasma density maximum at the axis and shifted from the axis. The transformation from an annular to axial shape was obtained in experiment [65] and confirmed in simulations [63, 64].

Numerical simulations of plasma chemistry in the atmospheric plasma jets, taking into account tens of species and hundreds of various reactions are being actively developed [66–70]. Simulations of the interaction of CAP with cell membranes in the vicinity of the skin wound were also conducted and efficiency of delivery of plasma products such as ions, reactive oxygen and nitrogen species onto cell membranes and ways to control these fluxes were studied.

2.4. Plasma interaction with liquids

One of the important aspects of plasma application in bioengineering and medicine is plasma interaction with liquids leading to chemical reactions that can produce various species in an aqueous solution.

In a recent paper 20 naturally occurring amino acids in an aqueous solution were studied using high-resolution mass spectrometry [71]. In particular it was found that chemical modifications of 14 amino acids can be observed after CAP treatment including (i) hydroxylation and nitration of aromatic rings in tyrosine, phenylalanine and tryptophan; (ii) sulfonation and disulfide linkage formation of thiol groups in cysteine; (iii) sulfoxidation of methionine and (iv) amidation and ring-opening of five-membered rings in histidine and proline. Concentration of amino acids after plasma treatment is shown in figure 7. The side chains of 14 amino acids were oxidized to form various products, and sulfur-containing and aromatic amino acids were preferentially decreased in a competitive plasma treatment experiment. This is a very important database that can provide fundamental information for elucidating the mechanism of protein inactivation for medical application of CAP. CAP-generated ROS/RNS diffuse into liquid where they react with the cells in cultured media [72]. Some of these reactions are summarized in figure 8.

The CAP interaction with the cell culture medium might lead to significant reduction of pH potentially leading to cell death. In particular, increasing doses of the cell culture medium with CAP might lead to a drop in pH from 8.5 to 5.5 with dose increases. From 5 to 30 J cm^{-2}, respectively [73]. Acidification of the liquid (cultural media) was often shown to be due to a CAP treatment, which was attributed

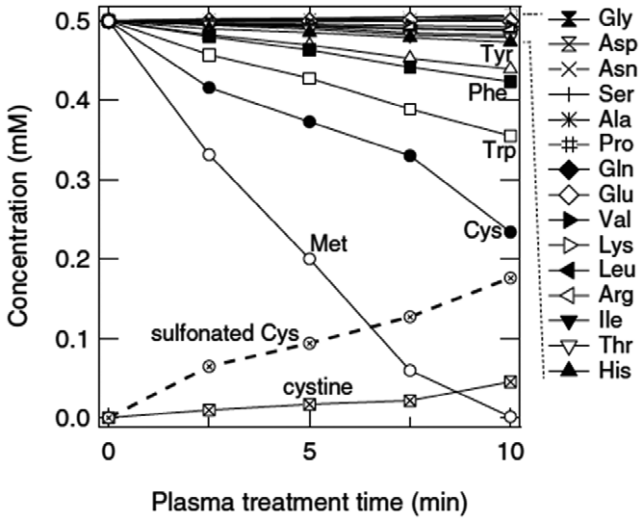

Figure 7. Comparison of plasma treatment effect on 20 amino acids. The prepared concentration of the amino acids was 0.5 mM. Note: the concentration of cysteine was also measured, and the concentration of sulfonated Cys was calculated from those of Cys and cystine. Published with permission from IOP [71].

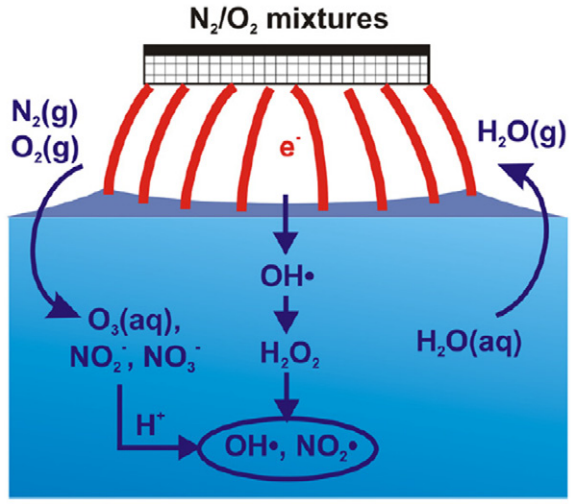

Figure 8. After Luces *et al*. Air plasma creates various ROS that end up in the water in the form of dissolved O_3, NO_2, NO_3, H, OH, H_2O_2, and NO_2. Published with permission from IOP [72].

to the multistep reaction of plasma-generated reactive species including NO, O, O_3 at the gas–water interface. On the other hand some authors argued that change of pH of the medium upon CAP treatment does not play a significant role [73].

3. Cold plasma effects *in vitro*

Significant efforts devoted to CAP application for bacterial deactivation build up a good understanding of the CAP biomedical potential. Stoffels *et al* [74] studied the plasma needle and demonstrated the non-thermal nature of the plasma interaction with cells. It was observed that plasma interacts with organic materials without causing thermal/electric damage to the surface, although this conclusion was not supported by direct measurements [75]. It became clear that CAP will play an increasing role in biomedical applications.

3.1. Cell migration

Several researchers observed that CAP application influences the cell motility [15–18, 76]. Cell migration is mediated by changes in cell–matrix interaction and cytoskeletal organization, and it is a key event controlling wound healing and metastasis of various cancers. A family of proteins called integrins play the role of mechanosensors to regulate cell migration. Integrins function as heterodimers of two subunits and there are over 18 different a and 8 different b chains that combine to form at least 24 different ab heterodimers [77]. Integrins are integral membrane proteins that bind extracellularly to the extracellular matrix and intracellularly to the actin cytoskeleton. Integrins can be expressed on cell surfaces with low affinity, inactive conformations, as well as with high affinity or active conformations with the regulation of their activation controlled by an increasing number of different cell signaling events. Studies examining cold plasma effects on cell migration found that cell migration rates and β_1 and α_v integrin expression are affected by plasma [78]. Cells dynamically adapt to forces by modifying their behavior and remodeling their environment. Adaptations include integrin clustering and activation and the formation of focal adhesion sites where cells bind to their substrate [79].

In one particular study the impact of CAP on integrin activation was carried out [18]. Immunofluorescent images are acquired and subjected to quantitative image analysis as described in the methods section. A photo of a typical set up *in vitro* is shown in figure 9(A). Figure 9 shows the results of immunofluorescence studies to assess the activation state of the β_1 integrin in the CAP treated fibroblasts. Untreated cells (control), cells treated with $MnCl_2$ only, CAP-treated (100 s) cells, and cells treated with plasma (100 s) and $MnCl_2$ are also illustrated in figure 9(A). An enlargement of the image shown in figure 9(B) is shown in figure 9(C). One can see that activated $\beta 1$ integrin is present at significantly higher amounts in cells treated with $MnCl_2$, CAP, and both CAP and $MnCl_2$ confirming that $\beta 1$ integrin is activated by CAP treatment (see figure 9(D)).

3.2. Cancer cell treatment

A substantial body of information has been accumulated with respect to application of CAP for cancer cell treatment *in vitro*. Initial studies were limited to skin cells and only simple cell responses to the cold plasma treatment were reported [80–83]. More recent work presents preliminary results on the *in vivo* treatment of U87 glioma-bearing mice [84]. It was demonstrated that cold plasma treatment of a U87-luc glioma tumor leads to a decrease of tumor bioluminescence intensity and tumor volume.

An important characteristic of CAP interaction with cancer cells is selectivity. In one example a significant selective effect of CAP was observed; namely about 60–70% of SW900 (lung cancer cell line) cells were detached from the plate in the zone treated with plasma [21], while no detachment was observed

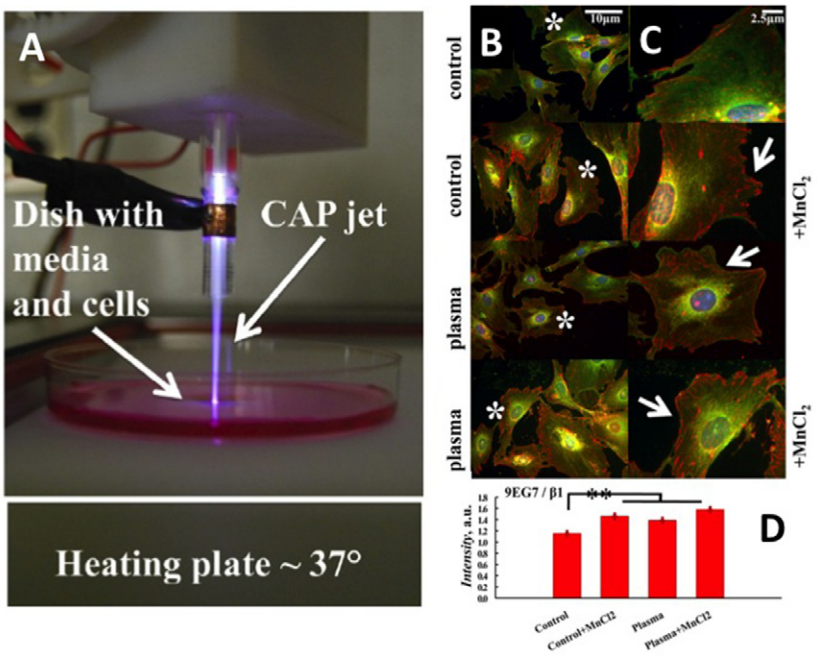

Figure 9. (A) Photo of a typical *in vitro* set up. (B)–(D) Activation of the β1 integrin with CAP. The immunofluorescence images of the fibroblast cells with different scales are shown: control (no treatments), control +$MnCl_2$ (treated with only $MnCl_2$), plasma (treated with CAP 100 s), plasma +$MnCl_2$ (treated with both plasma 100 s and $MnCl_2$). Total β1 integrin are shown in green, activated β1 (clone 9EG7) in red and nuclei in blue. (B) Images were taken with 20 × magnification. Cells enlarged in the figure 3(c) C are marked with the white asterisk. (C) Enlarged typical cells are shown. White arrows indicate the increase of the activated β1 integrin. (D) The data represent the ratio of 9EG7 and total β1 integrin for the peripheral part of the cells; error bars stand for with the standard error of mean, ~20 cells were analyzed per each conditional change. The double asterisk shows the statistical significance (p-value < 0.001) in the increase of the intensity of the 9EG7 over the total β1 in the cells treated with $MnCl_2$, plasma or both (with permission from IOP [18]).

in the treated zone for the NHBE (normal lung) cells under same treatment conditions, as shown in figure 10. One can notice that the CAP treatment leads to a significant reduction in SW900 cell count, while NHBE cell count is practically unchanged as shown in figure 10.

CAP treatment leads to integrin activation [18] and the downregulation of E-cadherin and the EGF receptor has been observed in human keratinocytes [85]. These effects significantly alter cellular motility [16–18]. While most studies were performed for fibroblasts, one can imagine significant implications for cancer research, since cell migration plays an important role in tumour growth and metastasis. Indeed recently it was shown that human metastatic breast cancer (BrCa) cells and bone marrow derived human mesenchymal stem cells (MSCs) respond very differently to CAP treatment [86]. BrCa cells were more sensitive to CAP treatments than MSCs under the same plasma dose. CAP selectively targets metastatic BrCa cells without damaging healthy MSCs at the metastatic bone site. In addition, it was obtained that CAP treatment inhibits the migration and invasion of BrCa cells.

In a recent study, head and neck squamous cell carcinoma (HNSCC) treatment by CAP was studied. Four HNSCC cell lines (JHU-022, JHU-028, JHU-029, SCC25) and two normal oral cavity epithelial cell lines (OKF6 and NOKsi) were subjected to CAP for durations of 10, 30 and 45 s [87]. HNSCC cell viability was altered in a dose-response manner, as evidenced by MTT assays; the viability of the OKF6 cells was not affected by the cold plasma. The results of colony formation assays also revealed a cell-specific response to CAP application.

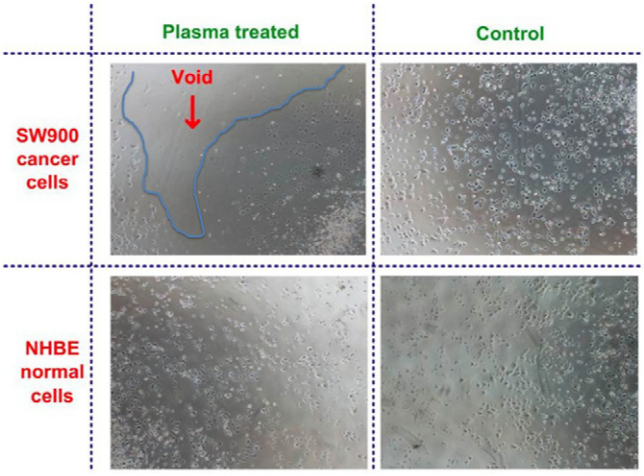

Figure 10. Selectivity effect of plasma treatment: SW900 cancer cells were detached from the plate in the zone treated with plasma, while no detachment was observed in the treated zone for the normal NHBE cells. Cells were treated for 30 s with CAP. Published with permission from *Br. J. Cancer* 2011 [21].

In one of the first experiments related to CAP interaction with cancer cells it was shown that plasma treatment time is an important factor, as shown in figure 11(a). One can see that CAP leads to cancer cell death [88] and what is surprising is that even 24 h following treatment, the total cell number continues to decrease as shown in figure 11(a). CAP induced a major decrease in cell number as compared to control as shown in figure 11(b). In the U87MG cell line, a 10 J cm^{-2}

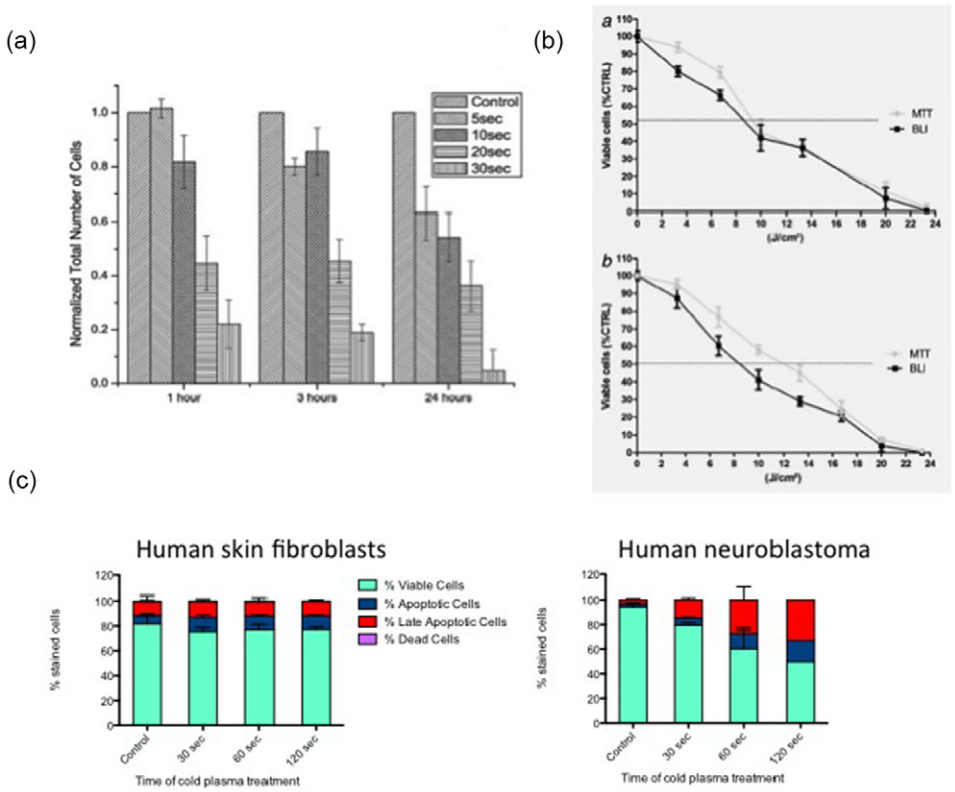

Figure 11. (a) Plasma treatment effect on melanoma cancer cells (Plos One [88]). (b) Plasma treatment effect on U87MG (a) and HCT-116 (b) cells. Cell viability was determined 24 h after treatment by both MTT and BLI assays. Cell viability of CAP-treated cells was normalized to untreated cells. (Published with permission from *Int. J Cancer* [22]), (c) Selectivity effect of plasma treatment: fibroblast cells treated with the cold plasma device for 0, 30, 60 and 120 s. Annexin and 7-AAD staining was performed for flow cytometry analysis at 48 h after treatment. Four-quadrant analysis of the results characterizes the cells as viable (unstained), apoptotic (Annexin positive), late-apoptotic (double positive), and dead (7-AAD positive). (Published with permission from AIP, 2013 [26]).

treatment induced a 46% significant decrease in living cells associated to 312% significant increase in dead cells. Using 20 J cm^{-2}, almost all cells were dead after 24 h. Figure 11(c) shows a clear-dose response to CAP treatment in the neuroblastoma cells at both 24 and 48 h, while the treated fibroblast cells do not differ from control at either 24 or 48 h [26, 89].

The effects of CAP on leukemia cells was also investigated [19]. These cells are non-adherent and typically found suspended in solution making them suitable for investigation of CAP treatment in solution. The authors suggested that leukemia cells suspended in a growth solution, and treated in that solution, simulates an environment more closely to the natural environment. It is very promising that CAP treatment also displays the dose response to the killing curve using the leukemia cells *in vitro* as shown in figure 12.

Several studies demonstrated the effects of the plasma-treated media on cancer cells. In one study glioblastoma (GBM) brain tumor cells and normal astrocytes were treated with media that was treated with CAP or plasma-activated medium PAM [90]. It was concluded that the glioblastoma cells were selectively killed by PAM and that PAM induced morphological changes consistent with apoptosis in glioblastoma. An apoptotic pathway was confirmed by using an apoptotic molecular marker, cleaved Caspase3/7. It was also found that PAM downregulated the expression of AKT kinase, a marker molecule in a survival signal transduction pathway. It was pointed out that the killing capability of CAP-stimulated media can be controlled by regulating the concentration of fetal bovine serum (FBS) in media and the store temperature for stimulated media [91]. FBS and Dulbecco's modified eagle's medium (DMEM) in the stimulated media play opposite roles in determining the ultimate fate of glioblastoma cells [91].

In a recent study [92] the effect of CAP on the T98G brain cancer cell line was studied. It was shown that after the plasma treatment, only a fraction of the seeded cells retained the capacity to produce colonies among living cells. These results indicate that CAP was not only inducing death in T98G cells, but also significantly affecting the reproductive capacity of the cells, indicating possible genetic damage.

It is recognized that intratumoral heterogeneity challenges existing paradigms for anti-cancer therapy [93]. In particular, cancer stem cells are the most resistant population and are responsible for tumor recurrence and metastasis. In this respect a recent study of CAP treatment of three different ovarian cancer stem cells is of great importance. Initial *in vitro* results showed that all three cells lines considered were sensitive to plasma to varying degrees. The C12 cell line was very sensitive to the plasma treatment, the other two (C13 and C13diff) to a lesser degree.

In summary, it was shown that CAP interaction with various cancer cell lines and normal cells leads to selective killing of cancer cells. CAP is effective in many different types of

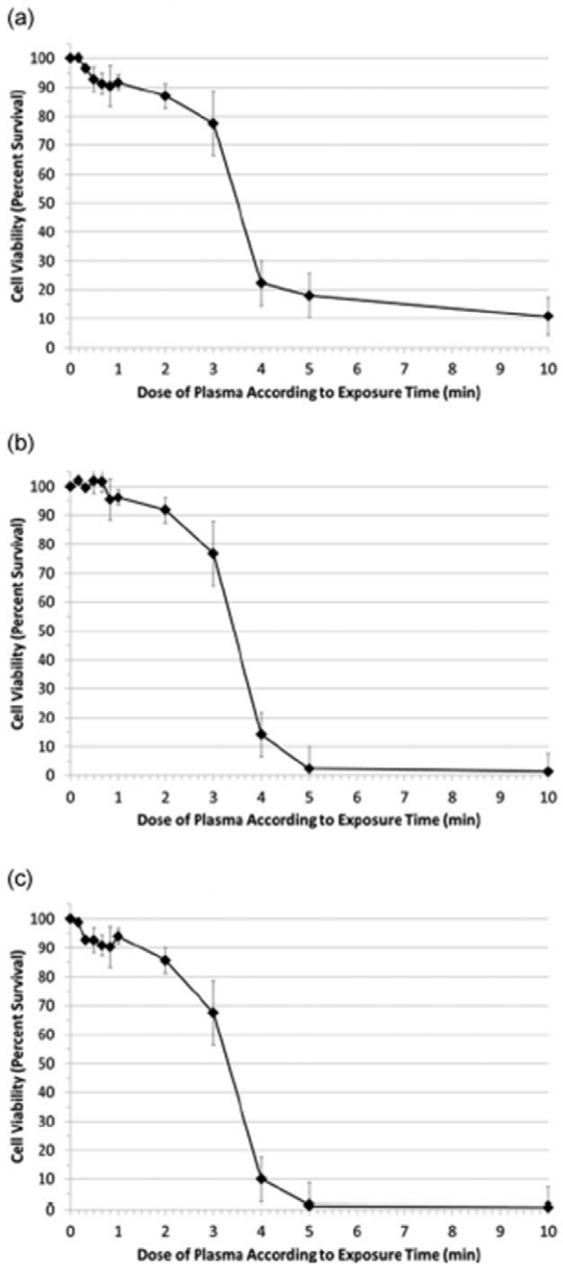

Figure 12. After Barekzi and Laroussi [19]. The effect of different plasma exposures on the viability of CCRF-CEM leukemia cells. (a) Percentage of viable cells at 12 h post-plasma treatment, (b) Percentage of viable cells at 36 h post-plasma treatment, (c) Percentage of viable cells at 60 h post-plasma treatment. Published with permission from IOP [19].

cancer indicating that the effects of plasma seems to be uniform and are not restricted to a particular tumor type [19, 73, 94]. In the next section we present results and analysis of CAP application *in vivo*.

4. Cold plasma effect *in vivo*

The first *in vivo* demonstration of CAP anti-cancer potential was done by Vandamme *et al* [20]. Human U87 glioblastoma xenotransplants were used in that study. It was shown that treatment over multiple days has been effective in reducing tumor volume and increasing survival time as shown in figures 13(A) and (B). Plasma was applied each day over five-consecutive days on subcutaneously U87MG-Luc grafted tumors. To determine the effect of NTP on tumor cell proliferation and metabolism, BLI was performed before (D0), during (D3) and after (D5) the treatment course (see figure 13(A)). In non-treated and treated mice groups, BLI activity showed three fold increase between D0 and D3. Tumor volume measurements performed 24 h after the end of the treatment course (figure 13(B)) revealed a significantly lower tumor volume in the treated group compared to-control. It was argued that observed effects are related to ROS-mediated apoptosis.

The anti-tumor action of CAP was demonstrated on a syngenic mouse melanoma and a heterotopic human bladder cancer xenograft models [21]. In this series of work the CAP was applied to nude mice bearing subcutaneous bladder cancer tumors (SCaBER). The set up of the typical *in vivo* experiment is shown in figure 14. The ability of CAP to ablate the tumor in a single treatment was one of the most interesting results demonstrated. In particular, tumors of about 5 mm in diameter were ablated after about 2 min of a single treatment. Recall that fully ablated tumors did not grow back while partially destroyed tumors started growing back a week after treatment, although it should be pointed out that they did not reach the original size even three weeks after treatment. In addition a murine melanoma model was employed to evaluate the CAP anti-tumor action [21]. Similarly, CAP treatment of a transcutaneous tumor led to ablation. One can see the effect of the CAP treatment in figure 13(C); in which tumor growth rates markedly decrease. CAP treatment resulted a significantly improved chance of survival in the treatment group ($p = 0.0067$), with a median survival of 33.5 d versus 24.5 d, as shown in figure 13(D).

Overall it was demonstrated by several authors that CAP causes a significant reduction of tumor size and a consecutive elongation of survival time. The CAP *in vivo* action was also confirmed in a heterotopic mouse model using neuroblastoma cells [83] and in an orthotopic pancreas carcinoma model [95]. Several groups developed hybrid approaches including CAP treatment and chemotherapy. In one case GBM cancer cells were studied *in vitro* by applying the alkylating agent temozolomide (TMZ) and CAP [96]. It was shown that CAP treatment restored the responsiveness of resistant glioma cells towards TMZ therapy as shown in figure 15(A). *In vivo* studies of combined therapy for the case of pancreatic tumors were also performed [95]. Over a 36 day period, it was demonstrated that CAP in conjunction with chemotherapy drug induced an inhibition of cancer cell proliferation *in vitro* and *in vivo*. When combining CAP and the drug gemcitabine (GEM), BLI intensity was significantly lower than in the control group. On day 36, a significant difference of tumor volumes and weight was observed for the group treated with the bi-therapy (the NTP + GEM group) as compared to the control group (see figure 15(B)). It was concluded from these observations that the CAP antitumor effect increased by 33% when it is associated with gemcitabine.

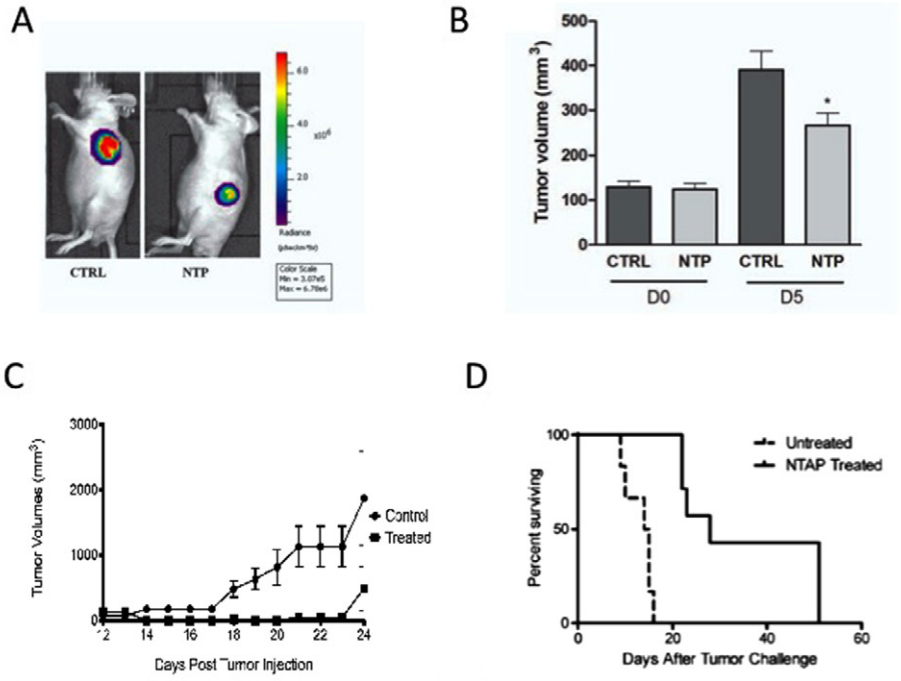

Figure 13. CAP treatment *in vivo*. (A) Representative BLI imaging of control and plasma treated mice. (B) Tumor volume determined by a caliper 24 h after the last day of treatment (day 5). (Published with permission from *Br. J. Cancer* 2011 [21]), (C) Effect on the growth of established tumor in a murine melanoma model. (Published with permission from *Br. J. Cancer* 2011 [21]), (D) CAP treatment effect on the mice survival in a murine melanoma model. (Published with permission from *Br. J. Cancer* 2011 [21].)

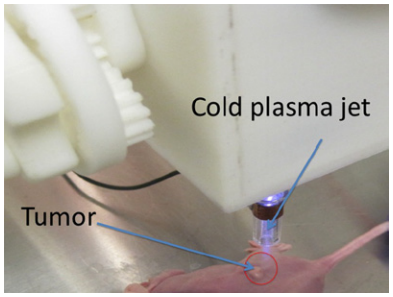

Figure 14. Cold plasma device and typical image of CAP treatment of a single tumor. Published with permission from *AIP* [26].

CAP is able to successfully trigger ROS production in tumors. Recent results show that the elevated ROS level seen with flow cytometry in the top third of a 10 mm tumor indicates that the maximum penetration seen with our device would be about 3 mm [97]. This is consistent with other reporter molecules showing that plasma can deliver ROS from 150 μm to 1.5 mm below the tissue surface across the 'model tissue' [98].

Very important observations regarding oxygen pressure measurements were reported recently [99]. Tissue oxygen partial pressure (pO2) was measured using a time-resolved luminescence-based optical probe. A rather rapid oxygen pressure increase (up to four times) was subcutaneously measured during CAP treatment and this increase was correlated with blood flow improvement. It should be noted that oxygenation and perfusion could open new opportunities for tumor treatments in combination with radiotherapy.

5. Effect of CAP on cell cycle

According to conventional wisdom a way to target cancer cells is to interfere with the cell cycle [100–102]. It stems from the fact that cancer cells proliferate at a faster rate than normal cells [103]. There are several studies suggesting that CAP interaction with cells, particularly cancer cells, leads to modifications in the cell cycle. In fact recent data confirmed that cancer cells are more susceptible to the effects of CAP because a greater percentage of cells are in the S-phase [27].

Recall that one of the hallmarks of cancer treatment is the approach to deregulate the mechanisms controlling cell cycle [104]. Note that the cell cycle or 'life of cell' outlines the different stages taking place as a cell develops. In particular, DNA synthesis occurs during the specific period of the cell cycle, which is called the S-phase Morphological changes in cell refer to the mitotic phase (M-phase); a phase of the cell division. The stages between M and S and between S and M phases are called the G1 and G2 phases. It should be pointed out that non-proliferating cells are in the G1 phase of the cell cycle. Once cells proliferate, they move progressively from G1 to S (i.e. the synthesis of DNA), to G2, and then the M (mitosis) phase where they divide. Cells in G1 can be either in quiescence (G0), terminally differentiate, or, in response to specific signals, be induced to proliferate. Most cells in normal adult tissues are in a quiescent G0 phase. Between S and G2 and between G2 and M phases there are so-called 'checkpoints'. Cell progression through the cell cycle is monitored and controlled by these checkpoints. Checkpoints verify

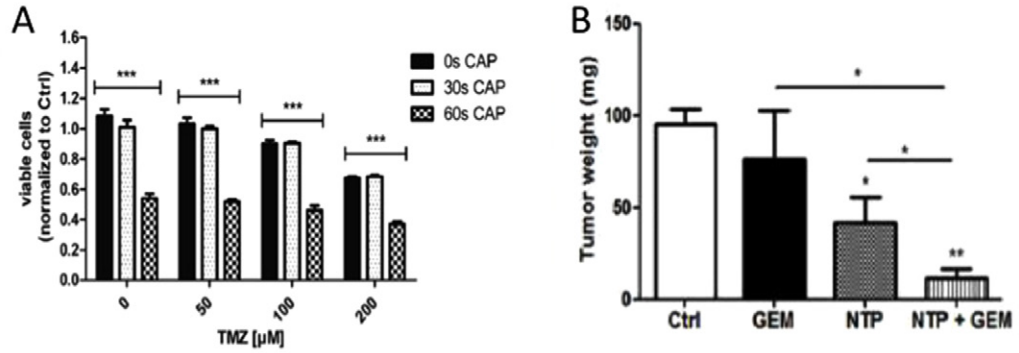

Figure 15. Combined treatment using CAP and chemotherapy. (A) Combined treatment of glioma cells with TMZ and CAP. U87MG cells were CAP treated once and TMZ was applied consecutively afterwards for three days [96]. (B) Plasma gun and gemcitabine treatments effects on tumor growth in an orthotopic pancreatic model. Three days after tumor induction, mice were randomly assigned into four groups: control (CTRL), gemcitabine (GEM), plasma gun (NTP) and bi-therapy (NTP + GEM); there were eight mice per group. Tumor weight at the end of the study is shown [95]. Published with permission from *PloS One*.

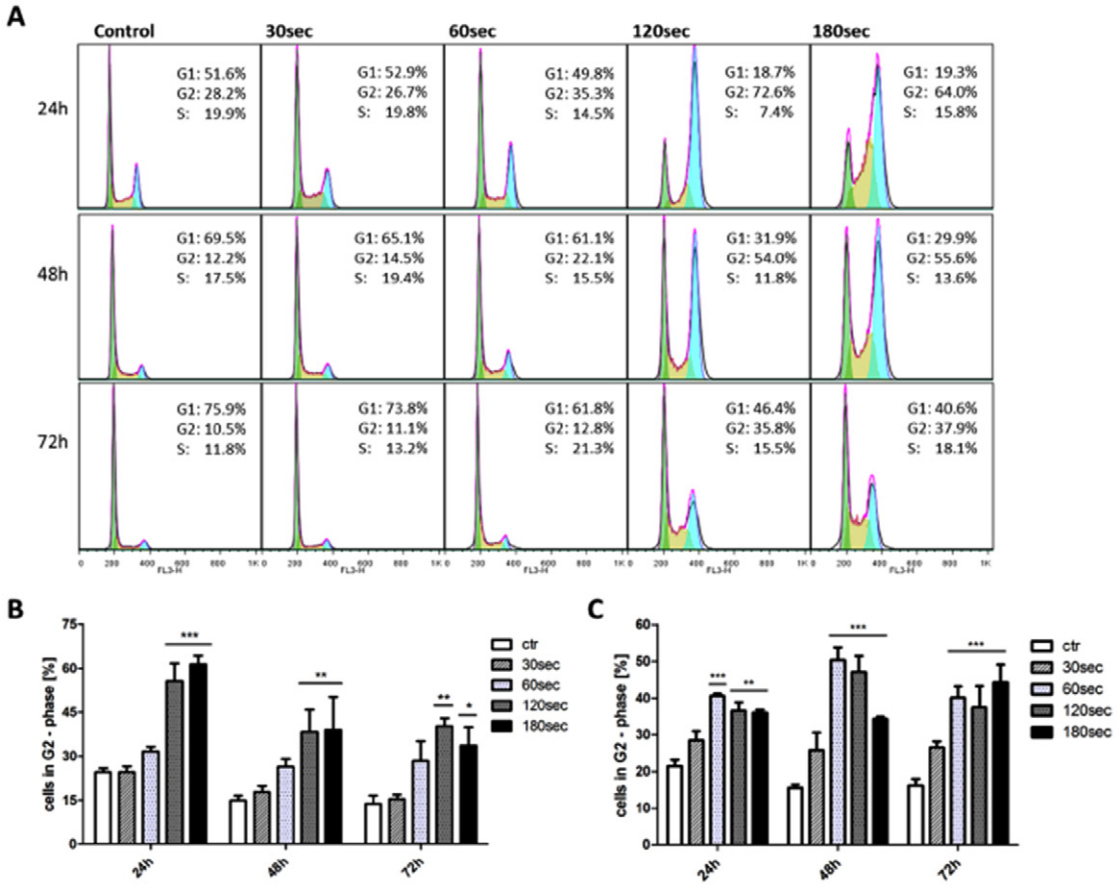

Figure 16. After Koritzer *et al* [96]. Cell cycle arrest in G2/M-phase. (A) Cell cycle analysis of U87MG cells was performed 24, 48 and 72 h after CAP treatment (30, 60, 120 and 180 s) by flow cytometry. Treatment was performed only with a thin film of liquid covering the cells. (B) Statistical significances of the observed arrest in the G2/Mphase in U87MG; (C) Statistical significances of the observed arrest in the G2/Mphase in U87MG in LN18 cells. Published with permission from *PloS One* [96].

whether the processes at each phase of the cell cycle have been accurately completed before moving into the next phase.

Initial analysis of CAP effect on glioblastoma [96] suggested that the CAP treatment causes significant arrest in the G2/Mphase in U87MG cells. It was found that this effect depends on plasma dose. To this end the cell cycle progression of LN18 and U87MG glioma cells 24, 48 and 72 h after CAP exposure was analyzed and results are shown in figure 16. Treatment of glioma cells with CAP for 120 and 180 s led to a two-to-four times higher number of cells in the G2/M-phase of the cell cycle compared to the untreated control. This significant arrest was observable for at least 72 h (figures 16(B) and (C)). In these studies no sub-G1 population was observed in cells treated for up to 180 s, further confirming the

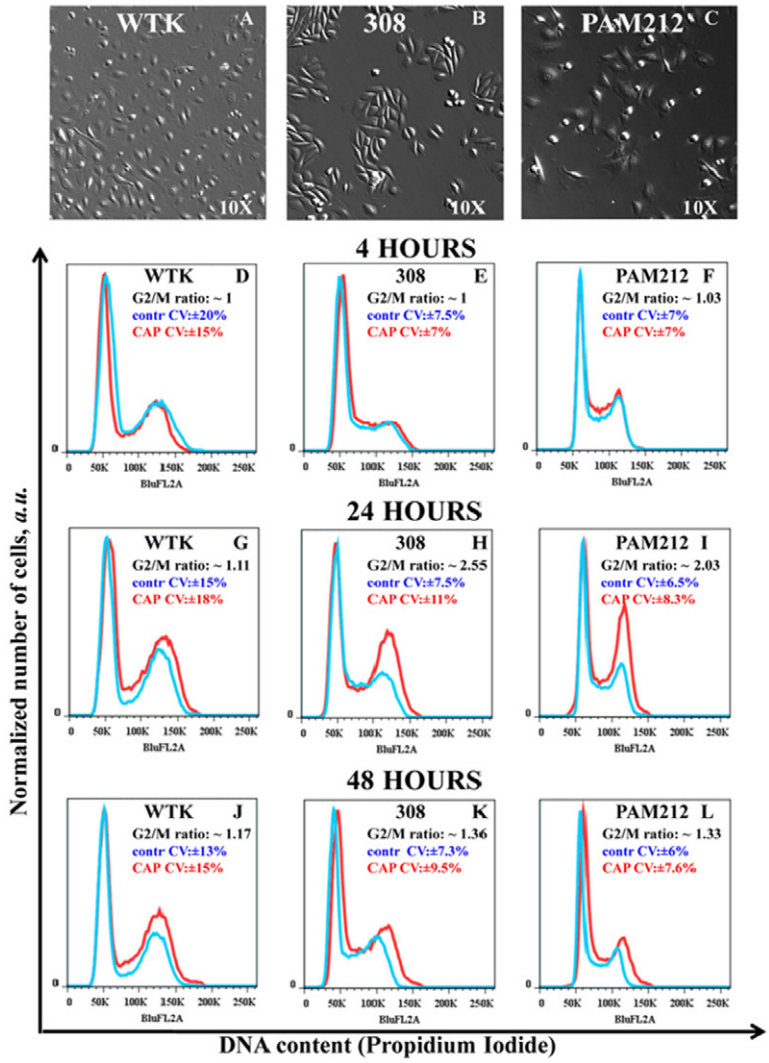

Figure 17. Identification of the cell cycle change in G2/M-phase. (A)–(C) Bright-field images of wild type keratinocytes (WTK), epidermal papilloma (308 cells) and epidermal carcinoma (PAM212 cells) cells are shown with a 10 × magnification. (D)–(L) show cell cycle studies: propidium iodide content (horizontal axis) and normalized number of cells (vertical axis) are shown. The controls are shown in blue and cells CAP treated for 60 s are in red. The ratio of the number of cells (treated to untreated) in G2/M-phase with coefficients of variation (CV, in percents) is shown in the right top corner of each figure. (D)–(F) shows cell cycle measurements in about 4 h; (G)–(I) in about 24 h; and figure (J)–(L) in about 48 h after the CAP treatment for WTK, 308 and PAM 212 cells respectively. Reprinted with permission from [27]. Copyright (2012) by Macmillan Publishers Ltd.

cytostatic effect as more prominent than the apoptotic effect of CAP on glioma cells [96]. Vandamme *et al* [22] also found that in U87MG cells, plasma treatment led to a significant decrease of number of cells in G0/G1 phase with a significant increase of cells in S-phase.

The effect of CAP treatment on cell cycle was studied for three different cell lines [27]. Bright-field images with 10 × magnification of wild type keratinocytes, 308 and PAM212 cells morphology, respectively, are shown in figure 17. Figures 17(D)–(L) are DNA content measurement of control (untreated) cells in blue, and cells treated with CAP for 60 s in red. The cells were investigated after 4 and 24 h after CAP treatment (60 s). One can see that no significant shifts in the G1–G2 peaks positions were observed for all cell types considered. It can be seen that CAP induced robust G2/M-cell cycle increases in both carcinoma and papilloma cells (it is about 2–3-fold increase in about 24 h after CAP treatment), whereas normal keratinocytes showed almost no variation. It should be pointed out that this change diminished in about 48 h.

Further studies reveal which phase of the cell cycle CAP impacts the most. An assessment of the expression of γH2A.X (pSer139) at different phases of the cell cycle was performed. γH2A.X (pSer139) is known to perform as an oxidative stress reporter of S-phase damage. This histone comprises about 2–25% of the evolutionarily conserved variant of histone H2A; it goes through a post-translational modification in response to ionizing radiation, UV-light or ROS [105, 106]. It should be pointed out that γH2A.X can be used in combination with EdU-labeling to determine if the oxidative stress is induced in S-phase [107]. Time-sensitive response of cancer cells (308) to CAP treatment including DNA content in cells, DNA replicating cells and γH2A.X expression is shown in figure 18. Figure 18(A) displays the EdU/DNA content

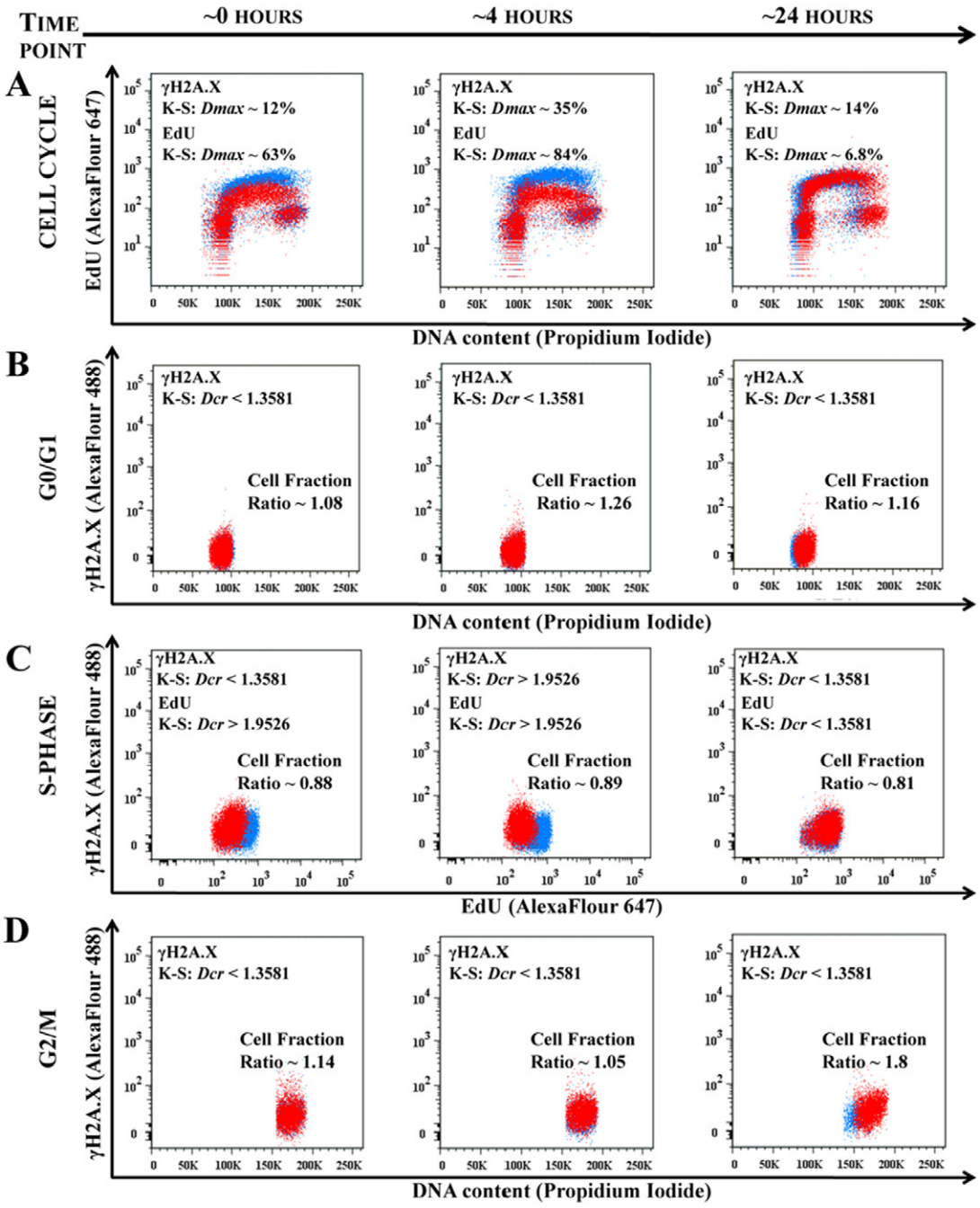

Figure 18. CAP targets the cell cycle phase. The time-sensitive studies of the cell cycles of the 308 cell line are shown for the time points ~0, ~4 and ~ 24 h after 60 s of CAP treatment. The control (not-treated cells) is shown in blue, CAP treated cells is in red. (A) shows the time evolution of the cell cycles (DNA content-versus-DNA replicating cells) of the control and CAP treated cells. The changes in EdU and γH2A.X signals are characterized by K–S maximum difference $D_{\max}$ and D_{cr} values at the selected time point. (B) shows the correlation between DNA content and γH2A.X reporter for G0/G1 cell phase; (C) shows correlation between DNA replicating cells (EdU) and γH2A.X for 308 cells in S-phase; and (D) shows correlation between DNA content and γH2A.X for the 308 for G2/M-phase for ~0, ~4 and ~24 h time points. About 25 000 cells are shown for each experimental condition. Changes in the fraction of cells between the control (not treated) and CAP treated cells are shown for each cell phase: cell number decreases if the ratio is less than one. The statistical description of the signals shown in the (A) is a maximum difference between two distributions in the S-phase with a confidence interval of 99.9%; in the (B)–(D) D_{cr} the value is shown: $D_{cr} < 1.3581$ ($p > 0.05$) is considered not statistically significant and $D_{cr} > 1.9526$ ($p < 0.001$) is extremely statistically significant. Reprinted with permission from [27]. Copyright (2012) by Macmillan Publishers Ltd.

immediately following, and at 4 and 24 h after CAP treatment. One can see a very significant change in the S-phase signal (EdU) immediately, and at about 4 h after treatment: almost a 2-fold decrease in the median value with decrease of variation range value, while still no significant changes were observed in G0/G1 and G2/M. After about 24 h the S-phase is recovered and the number of cells in G2/M stage was increased. Figures 18(B)–(D) shows the correlation between γH2A.X signal and DNA content in G0/G1-phase (B); with EdU incorporation to highlight S-phase cells (C), and with DNA content

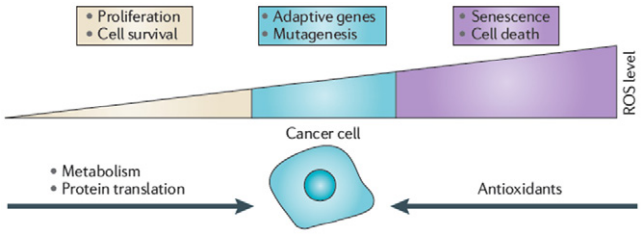

Figure 19. Relationship between the levels of ROS and cancer. Reprinted with permission from (Cairns R, Harris I and T W Mak, 2011 *Nat. Rev. Cancer* **11** 85–95). Copyright (2011) by Macmillan Publishers Ltd [110].

to highlight cells in G2/M-phase (D). It can be pointed out that there are no significant differences in γH2A.X (pSer139) expression in cells at G0/G1 at any time point. On the other hand there is an increase in γH2A.X (pSer139) expression, which is correlated with about a 2-fold decrease in the EdU-signal in cells mostly in the S-phase immediately (0 h) and 4 h after CAP treatment (as shown in figure 18(C)). Recall that the changes in γH2A.X (pSer139) expression are less apparent about 24 h after CAP treatment.

In summary, it was demonstrated that CAP selectively targets the cancer cells' cycle. Similarly to chemotherapy and radiotherapy, CAP selectivity is ensured by interfering with the mitotic cell cycle and inducing cell cycle arrest, DNA damage, and apoptosis via ATM expression and phosphorylation of p53. Based on these observations, higher sensitivity of cancer cells to CAP treatment can be explained by differences in the distribution of cancer cells and normal cells within the cell cycle. The selective effect of CAP suggest that, under the right conditions, CAP treatment will affect only cancer cells, while leaving normal cells essentially unharmed.

6. Molecular mechanisms of the cold atmospheric plasma-based anti-cancer treatment

Current understanding of the primary mechanism of CAP anti-cancer treatment is related to ROS and RNS production. Both ROS and RNS play a central role is 'redox' or oxidation–reduction biology [108]. These species are known as agents associated with various diseases including cancer. In the context of CAP treatment we will differentiate between intracellular and extracellular ROS and RNS.

Both ROS and RNS play an important role in biological systems. In a recent paper [109] Watson calls ROS 'a positive force for life' because of their role in apoptosis—an internal program that highly stressed cells use to induce death. On the other hand, ROS are also well known 'for their ability to irreversibly damage key proteins and nucleic acid molecules [i.e. DNA and RNA].' Under normal conditions, an excess of ROS is neutralized by an anti-oxidant system. It was pointed out that 'The vast majority of all agents used to directly kill cancer cells (ionizing radiation, most chemotherapeutic agents and some targeted therapies) work through either directly or indirectly generating reactive oxygen species that block key steps in the cell cycle.' This idea is illustrated in figure 19 in which the effect of ROS on cell fate is shown depending on

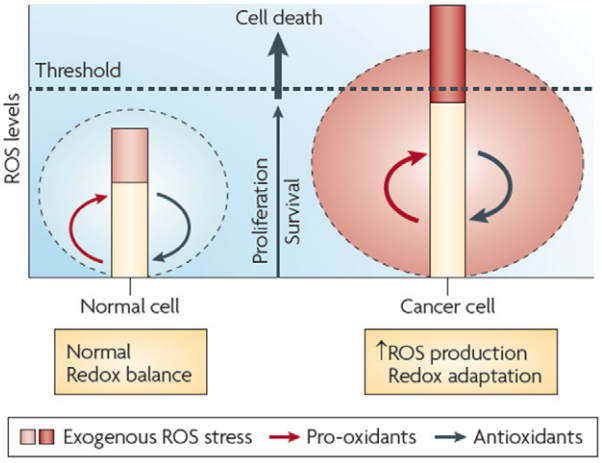

Figure 20. Schematics of selective targeting of cancer cells by ROS-based therapy. Reprinted with permission from [113]. Copyright (2009) by Macmillan Publishers Ltd.

the level of ROS [110]. It is shown that low levels of ROS provide a beneficial effect, supporting cell proliferation and survival pathways. On the other hand, when the level of ROS become excessively high it leads to oxidative stress that can end in cell death. In order to counter such oxidative stress, a cell uses antioxidants preventing ROS from accumulating at high levels.

It has been pointed out that in a cancer cell, aberrant metabolism generates abnormally high levels of ROS [110]. Additional mutations in a cancer cell leads to regulation of ROS and antioxidants helping cell survival. Such control of ROS allows the cancer cell to avoid the detrimental effects of high levels of ROS.

In a recent review article it was stressed that, while the main disadvantage of conventional therapies is the development of treatment-resistant cells, it is questionable whether or not cold plasma will lead to similar oxidative stress resistance [111]. It was hypothesized that combining nitrosative stress with oxidative stress via CAP might avoid such resistance development. There is significant evidence that NO and other related compounds can play a role of an agent that re-sensitizes tumors to chemotherapy and radiation therapy [111]. Indeed, CAP produces reactive nitrogen in addition to ROS and as such there is a hope that CAP will be able to overcome the issue with resistance.

It is known that significant increase in the intracellular ROS levels leads to DNA damage and apoptosis in the targeted cells [112, 113]. In fact, the levels of ROS in cancer cells are close to the limit at which cell death occurs and is much higher than in correspondent normal cells [113]. As such, the anti-cancer therapeutic approach is the use of ROS near the 'threshold' between levels of ROS in normal cells and cancer cells allowing the selectivity toward tumor cells. This approach is shown conceptually in figure 20 in which it is shown that normal cell survival is due to the low initial level of ROS while a higher level ROS in the case of a cancer cell leads to cell death.

A recent review of the current literature suggests that ROS might induce death of cancer cells by impairing the function of

Table 2. Properties of ROS/RNS.

	Formula	Biological half-life
Hydrogen peroxide	H_2O_2	~10^{-5} s
Superoxide	O_2	~10^{-6} s
Hydroxyl	OH	~10^{-9} s
Nitric oxide	NO	< 1 s
Peroxynitrite	$ONOO^-$	~1 s

intracellular regulatory factors [114]. In particular, it is plausible that that pro-oncogene, or tumor suppressor-dependent regulation of antioxidant/or ROS signaling pathways, may be involved in cancer cell death triggered by CAP.

With regards to above strategy, it was reported that CAP promotes generation of intracellular ROS inducing the apoptosis in DBD plasma-treated melanoma cells [73]. A variety of active neutral short- and long-lived ROS are formed in CAP including OH, O, electronically excited oxygen O (1D), O_2 ($1\Delta g$), O_3, HO_2, H_2O_2 [73]. RNS species such as NO_2^-, NO^- and NO^+ are induced directly in CAP [59] and through post-discharge processes in plasma-activated liquid mediated by peroxynitrite ($ONOO^-$). In addition, the peroxynitrite chemistry was also shown to significantly participate in the biological effects of CAP-activated liquid media [72].

Short-lived ROS generated by CAP might react with medium components (e.g. amino acids) to form long-lived reactive organic hydroperoxides [73]. These in turn might induce lipid peroxidation and cell membrane damage and activate intracellular signaling pathways resulting in apoptosis [112]. Exposure of cancer cells to CAP induces apoptosis in a caspase-dependent manner, and this effect is likely related to the production of ROS by CAP and DNA damage induced due to intracellular ROS [115]. ROS that are produced directly by CAP in air or in the media can subsequently diffuse into the cells through the cell's outer membrane or react with this membrane to produce intracellular ROS via lipid peroxidation. However, the diffusion time of ROS is typically larger than the corresponding biological half-life. Biological half-life times of the main components are shown in table 2 [116].

One can see that RNS have a significantly larger half-life and as such greater potential to be effective in CAP interaction with cells.

One possible pathway for reactive species interaction with cells is through interaction of RNS with mitochondria [73]. It is known that mitochondria are the major organelles that produce ROS and the main target of ROS-induced damage as observed in various pathological states, including aging. In particular NO plays a very important role through its interaction with components of the electron transport chain. NO might function not only as a physiological regulator of cell respiration, but also to augment the generation of reactive oxygen species by mitochondria, and thereby trigger mechanisms of cell survival or death. In mitochondria, ROS (primarily superoxide) is generated in three electron transport chain complexes (NADP-Q oxidoreductase, succinate-Q reductase, and Q-cytochrome oxidoreductase) [117]. As a counter process, superoxides can be eliminated by manganese (Mn)-dependent superoxide dismutase (MnSOD) in the matrix of mitochondria [73]. On the one hand, plasma-generated ROS/RNS might alter the anti-oxidation process. On the other hand, NO might inhibit the electron transport by attacking cytochrome c oxidase [118]. The interruption of electron transport will increases the generation of superoxide in matrix. In addition, the increasing superoxide reacts with NO to form peroxynitrite. Peroxynitrite can react with the key molecules in mitochondria, including mitochondrial DNA, mitochondrial membrane, and many mitochondrial protein components [119]. Among these molecules is MnSOD, which could be inactivated by peroxynitrite via 3-nitration on key tyrosine residue. As a result, the anti-oxidant system in mitochondria may be broken down after the interaction between RNS produced by CAP and mitochondria. In such a way the ROS stimulated by CAP might exert high oxidative stress on not only mitochondria but also cytoplasm. Indeed it was shown that enhanced ROS in the malignant cells (GBM, thyroid and oral carcinoma) led to death via alteration of total antioxidant activity, and $NADP^+$/NADPH and GSH/GSSG ratios 24 h post plasma treatment [120]. Similar effects were confirmed by annexin and propidium iodide staining. Kalghatgi *et al* [121] studied human breast cancer cells, and demonstrated dose-dependent apoptosis due to CAP effect. They analyzed the DNA damage using the phosphorylated histone variant H2AX and hypothesized that the cellular effects are mediated by peroxidation of amino acids in the cell culture medium. It was also determined that intracellular ROS may lead to mitochondrial dysfunction.

The overall possible process of CAP interaction with cell and consequent cell response is shown in figure 21. One can see that CAP treatment might lead to intracellular $ONOO^-$ and ROS increase. Both processes are correlated with apoptotic pathways [73, 122]. Note that this model presents a possible picture of CAP-triggered processes *in vitro*. There is still the question of how CAP interacts with tumors *in vivo*. One possibility is that ROS and RNS interact with the surface layer of cells and products of such interactions trigger cell–cell 'communication', which in radiation oncology is known as the 'bystander effect' [111].

CAP demonstrated its high selectivity toward p53-mutated cancer cells [123]. It was shown that the apoptotic effect of CAP was greater for p53-mutated cancer cells while artificial p53 expression in p53-negative HT29 cells decreased the pro-apoptotic effect of plasma treatment. They observed that CAP increases extracellular NO that did not affect cell viability while intracellular ROS increased under by CAP-induced apoptotic cell death. They concluded that CAP has great potential as a selective anti-cancer treatment, especially for p53-mutated cancer cells.

In a recent study, neuroblastoma cells subjected to CAP demonstrated an increased level in ROS following CAP treatment. It was determined that neuroblastoma cells enter apoptosis in a dose-dependent fashion in response to CAP treatment, while immortalized non-neoplastic cells are less sensitive to CAP. It was also shown that the pretreatment with ROS scavengers inhibited the induction of apoptosis by CAP, suggesting that ROS play a critical role in the cytotoxic effect. An *in vivo* study revealed that the elevated ROS level

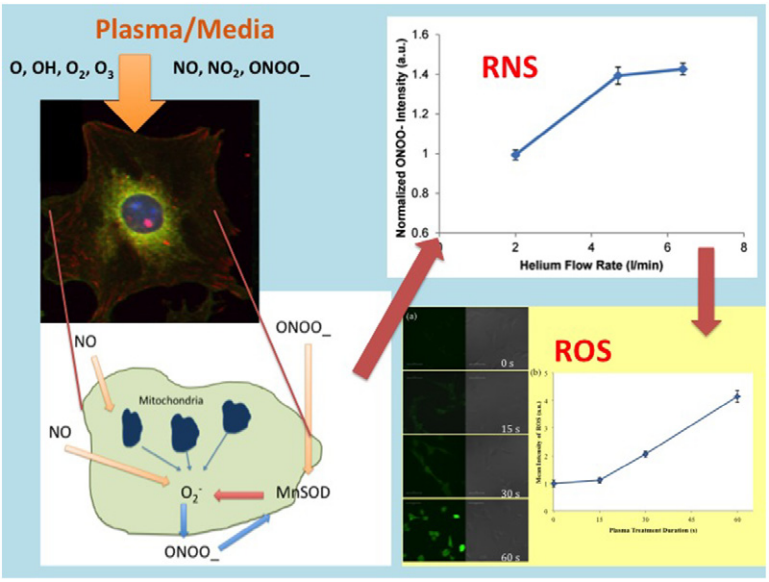

Figure 21. Schematics of CAP interaction with cells. NO and $ONOO^-$ can penetrate the membranes of cells and organelles. The electron transport chain in mitochondria might be blocked by NO. As a result, ROS production in mitochondria rises and ultimately damages mitochondria and trigger apoptosis. On the other hand, NO reacts with O_2^- generated in mitochondria to form peroxynitrite, which will attack nearly all important macromolecules in cells altering the antioxidant activity. Inserts show intracellular measurements of RNS and ROS.

seen with flow cytometry in the top third of a 10 mm tumor indicates that the maximum penetration seen with our device was about 3 mm [89, 97].

It was shown above that plasma interaction with living cells might trigger internal cell signals responsible for cell adhesion, proliferation or apoptotic death. Similarly conventional radiotherapy is widely used as one of the most powerful antitumor treatment methods. It aims to kill tumors by inducing apoptosis in cancer cells. It is well known that exposure to ionizing radiation affects DNA by inducing single and double strand breaks. Depending on the dose, ROS produced by ionizing radiation mediate either adaptive protective responses or genomic instability in irradiated cells [124]. Thus, at low doses of radiation, the oxidative DNA damage are counteracted by up-regulating DNA repair mechanism and antioxidant systems. Ionizing radiation exposure induces a transient 'oxidative burst' through water radiolysis that generates H_2O_2, which in turn causes DNA damage and mediates part of the radiation effect [124].

It should be pointed out that further progress in understanding molecular aspects of CAP anti-cancer modality is related to the ability to separate the effects of individual constituents along with synergistic effects of different CAP components.

7. Synergetic effect of plasma nanoparticles

A recent perspective article offered the suggestion that the synergetic effects of nanotechnology and CAP technology could lead to strong benefits for plasma-based medicine [125]. In fact, the nanoparticle-based cancer treatment approach led to the development of special antibody-conjugated gold nanoparticles, which can target cancer cells. Kim *et al* [126] achieved a five-fold increase in melanoma cell death with the use of CAP alone by using air plasma with gold nanoparticles bound to anti-FAK antibodies as shown in figure 22(A). It is known that FAK is a major signaling mediator. However, the authors argued that it is not clear which signal leads to cell death. Nonetheless, these results suggest that it is possible to achieve a precise attack against cancer cells using plasma and functionalized conjugates made of gold nanoparticles.

In a recent paper, synergy between gold nanoparticles and CAP in cancer therapy [127, 131] was demonstrated. In particular, it was shown that the concentration of gold nano particles (AuNPs) plays an important role. At an optimal concentration, gold nanoparticles in combination with CAP can significantly promote GBM (U87) cell death. One can see U87 cells' viability decrease by 30% in comparison with control group having the same plasma dosage but no AuNPs applied (figure 22(B)). The ROS intensity of the corresponding conditions has a reversed trend compared to cell viability. This result correlates well with the theory that intracellular ROS accumulation results in oxidative stress, which further changes the intracellular pathways, causing damage to the proteins, lipids and DNA.

8. Simulations of CAP interaction with tumors

The mechanism of CAP interaction with tumors is still elusive as demonstrated above. At the same time, mechanisms underlying tumor development, its progression and control are yet to be fully understood. With this in mind a new field of computational oncology emerges to utilize various simulation tools helping us to understand the cancer mechanism [128]. Naturally these are interdisciplinary efforts that include clinicians and biologists with mathematical and computational modelers and physicists. These simulations would have to take into account all of the mechanisms for

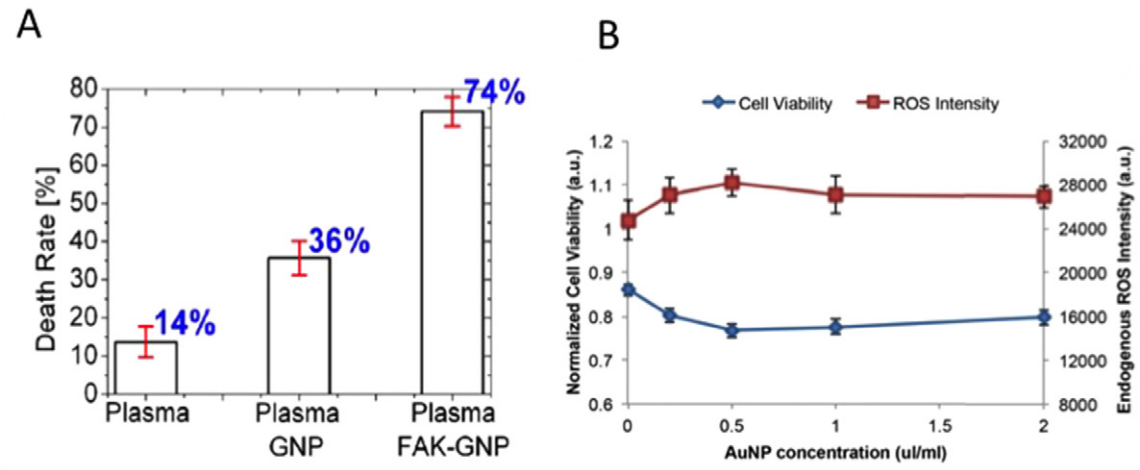

Figure 22. (A) After Kim *et al* [126]. Contribution of FAK-GNPs to dramatic G361 cell death with plasma irradiation. Comparison of the cell death rate which is significantly increased in the case of anti-FAK antibody-conjugated gold nanoparticles. (B) After Cheng *et al* [127]. Cell viability after 24 h incubation time with AuNPs after plasma treatment. Blue line: cell viability measured by MTT assay. Red line: intracellular ROS intensity measured by CM H2DCFDA probe. Reprinted with permission from IOP.

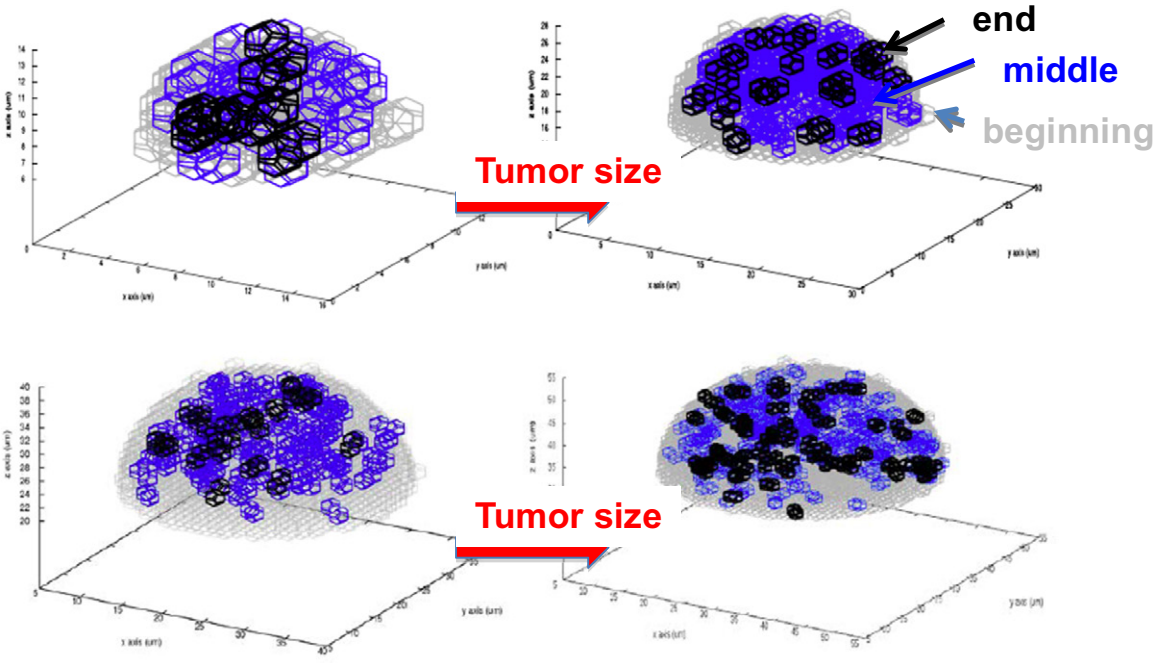

Figure 23. 3D model of tumor evolution under CAP treatment. Going from left to right and top to bottom we see four graphs of tumor morphology. Each simulation represents three time delineations from the initial tumor (gray), the midway treatment tumor (blue) and near the end tumor (black). (From [130], published with permission from IOP.)

tumor death and tumor growth to create predictions that can be verified with experimental data. Such an interdisciplinary approach promises to shed light on the intra-, inter- and extracellular mechanisms behind complex tumor dynamics [127]. Simulations and modeling are important for creating a personalized medicine, a new form of therapy that creates a personal treatment plan for a given tumor. Personalized medicine that includes simulations is the future of medicine allowing us to create more effective and more efficient targeted cancer therapies.

Recently a computational model of CAP interaction with a tumor was proposed [129]. The idea was to simulate a tumor that had been exposed to the CAP treatment. This includes simulating the apoptotic cell death that occurs from plasma treatment, normal cell growth and normal cell death. Tumor modeling entails use of the mathematical and physical equations to describe biological disease, most importantly the uncontrolled cell growth and tumor life cycle [130]. The model utilized a 3D hybrid discrete-continuum formulation. It was shown that CAP has a critical dosage, in which it will induce apoptosis selectively for cancerous cells while leaving healthy cells relatively unharmed, by using two separately calculated equations for the cancerous and healthy phenotype cells. Some results are shown in figure 23.

One can see from figure 23 that at the initial and halfway mark, the plasma-stimulated species have not fully diffused so the highest concentration of species is on the outer edge of the tumor. The probability of cell death is thus heavily dependent on both the species fluxes and a stochastic death function. This creates a more uniform cell death on the outer edges. The diffusion of ROS becomes more and more uniform with time. As a result it is apparent that when comparing the mid-treatment distribution and the final distribution, cell death is more sporadic. This is indicative of the shift of the cell death probability from a mixed continuous/stochastic function to just a stochastic function.

9. Summary

In summary, convincing evidence of CAP selectivity towards cancer cells has been accumulated. Various aspects of CAP application to cancer were studied worldwide including role of reactive species (reactive oxygen and nitrogen), cell cycle modification, *in vivo* application and CAP interaction with cancer cells in conjunction with nanoparticles. The two best known cold plasma effects, namely plasma-induced apoptosis and the decrease of cell migration velocity, have important implications in cancer therapy. CAP treatment can lead to localizing the cancer-affected area of the tissue and by decreasing the metastatic development. While mechanism of CAP action remains elusive, such promising results warrant further research in this exciting field.

Acknowledgments

The author would like to thank co-authors and collaborators Dayun Yan, Xiaoqian Cheng, Edward Ratovitsky, Alexey Shashurin, William Murphy, Caitlin Carroll, Olga Volotskova, Jonathan Sherman, Mary Ann Stepp, Grace Zhang (all from George Washington University), Barry Trink (Rambam Medical Center, Israel), Mikhail Shneyder (Princeton University), Jerome Canady (Institute for Advanced Biological and Technical Sciences, USMI), Anthony Sandler (Childrens' Hospital, DC) who contributed to some original results used in this review. This work was supported in part by a Dr Cyrus and Myrtle Katzen Cancer Research Center grant.

References

[1] Laroussi M, Kong M, Morfill G and Stolz W (ed) 2012 *Plasma Medicine* (Cambridge: Cambridge University Press)
[2] Fridman A and Friedman G 2013 *Plasma Medicine* (New York: Wiley)
[3] Keidar M and Beilis I I 2013 *Plasma Engineering: Application in Aerospace, Nanotechnology and Bionanotechnology* (Oxford: Elsevier)
[4] Stoffels E, Kieft I E, Sladek R E J, Van den Bedem L J M, Van der Laan E P and Steinbuch M 2006 Plasma needle for *in vivo* medical treatment: recent developments and perspectives *Plasma Sources Sci. Technol*. **15** S169–80
[5] Lakhovsky G 1929 *The Secret of Life: Electricity, Radiation and Your Body*
[6] Morrison J 1977 Electrosurgical method and apparatus for initiating an electrical discharge in an inert gas flow *US Patent* 4, 040, 426
[7] Lakhovsky G 1934 Multiple wave oscillator *US Patent* 1962565
[8] Fridman G, Friedman G, Gutsol A, Shekhter A B, Vasilets V N and Fridman A 2008 Applied plasma medicine *Plasma Process. Polym*. **5** 503
[9] Shashurin A, Scott D, Zhuang T, Canady J, Beilis I I and Keidar M Electric discharge during electrosurgery *Sci. Rep.* **4** 9946
[10] Stalder K R *et al* 2001 Electrosurgical plasmas *J. Phys. D: Appl. Phys.* **38** 1728
[11] Kong M G, Kroesen G, Morfill G, Nosenko T, Shimizu T, Van Dijk J and Zimmermann J L 2009 Plasma medicine: an introductory review *New J. Phys*. **11** 115012
[12] Morfill G E, Kong M G and Zimmermann J L 2009 Focus on plasma medicine *New J. Phys.* **11** 115011
[13] Stoffels E, Sakiyama Y and Graves D B 2008 Cold atmospheric plasma: charged species and their interactions with cells and tissues *IEEE Trans. Plasma Sci*. **36** 1441
[14] Kong M G, Keidar M and Ostrikov K 2011 Plasmas meet nanoparticles—where synergies can advance the frontier of medicine *J. Phys. D: Appl. Phys.* **44** 174018
[15] Shashurin A, Keidar M, Bronnikov S, Jurjus R A and Stepp M A 2008 *Appl. Phys. Lett*. **92** 181501
[16] Shashurin A, Stepp M A, Hawley T S, Pal-Ghosh S, Brieda L, Bronnikov S, Jurjus R A and Keidar M 2010 Influence of cold atmospheric jet on surface integrin expression of living cells *Plasma Process. Polym.* **7** 294–300
[17] Volotskova O, Shashurin A, Stepp M A, Pal-Ghosh S and Keidar M 2010 Plasma-controlled cell migration: localization of cold plasma-cell interaction region *Plasma Med.* **1** 83–93
[18] Volotskova O, Stepp M A and Keidar M 2012 Integrin activation by a cold atmospheric plasma jet *New J. Phys.* **14** 053019
[19] Barekzi N and Laroussi M 2012 *J. Phys. D: Appl. Phys.* **45** 422002
[20] Vandamme M, Robert E, Pesnel S, Barbosa E, Dozias S, Sobilo J, Lerondel S, Le Pape A and Pouvesle J M 2010 Antitumor effect of plasma treatment on U87 glioma xenografts: preliminary results *Plasma Process. Polym*. **7** 264
[21] Keidar M, Walk R, Shashurin A, Srinivasan P, Sandler A, Dasgupta S, Ravi R, Guerrero-Preston R and Trink B 2011 Cold plasma selectivity and the possibility of a paradigm shift in cancer therapy *Br. J. Cancer* **105** 1295
[22] Vandamme M *et al* 2011 ROS implication in a new antitumor strategy based on non-thermal plasma *Int. J. Cancer* **130** 2185
[23] Georgescu N and Lupu A R 2010 Tumoral and normal cells treatment with high-voltage pulsed cold atmospheric plasma jets *IEEE Trans. Plasma Sci*. **38** 1949–56
[24] Zirnheld J L, Zucker S N, DiSanto T M, Berezney R and Etemadi K 2010 Nonthermal plasma needle: development and targeting of melanoma cells *IEEE Trans. Plasma Sci*. **38** 948–52
[25] Kim J Y, Kim S O, Wei Y and Li J 2010 Flexible cold microplasma jet using biocompatible dielectric tubes for cancer therapy *Appl. Phys. Lett.* **96** 203701
[26] Keidar M, Shashurin A, Volotskova O, Stepp M A, Srinivasan P, Sandler A and Trink B 2013 Cold atmospheric plasma in cancer therapy *Phys. Plasmas* **20** 057101
[27] Volotskova O, Hawley T S, Stepp M A and Keidar M 2012 Targeting the cancer cell cycle by cold atmospheric plasma *Sci. Rep.* **2** 636
[28] Morfill1 G E, Shimizu T, Steffes B and Schmidt H-U 2009 Nosocomial infections—a new approach towards preventive medicine using plasmas *New J. Phys.* **11** 115019

[29] Weltmann K-D, Kindel E, Von Woedtke Th, Hähnel M, Stieber M and Brandenburg R 2010 *Pure Appl. Chem.* **82** 1223–37
[30] Lu X and Laroussi M 2006 *J. Appl. Phys.* **100** 063302
[31] Mericam-Bourdet N, Laroussi M, Begum A and Karakas E 2009 *J. Phys. D: Appl. Phys.* **42** 055207
[32] Sands B L, Ganguly B N and Tachibana K 2008 *Appl. Phys. Lett.* **92** 151503
[33] Ye R and Zheng W 2008 *Appl. Phys. Lett.* **93** 071502
[34] Begum A, Laroussi M and Pervez M R 2013 *AIP Adv.* **3** 062117
[35] Begum A, Laroussi M and Pervez M R 2011 *Int. J. Eng. Technol.* **11** 209
[36] Walsh J L, Iza F and Kong M G 2010 *Eur. Phys. J.* D **60** 523
[37] Walsh J L, Iza F, Janson N B, Law V J and Kong M G 2010 *J. Phys. D: Appl. Phys.* **43** 075201
[38] Kong M G, Ganguly B N and Hicks R F 2012 *Plasma Sources Sci. Technol.* **21** 030201
[39] Belostotskiy S G, Donnelly V M, Economou D J and Sadeghi N 2009 *IEEE Trans. Plasma Sci.* **37** 852
[40] Donnelly V M, Belostotskiy S G, Economou D J and Sadeghi N 2010 *J. Phys. Conf. Ser.* **227** 012011
[41] Wang Q, Koleva I, Donnelly V M and Economou D J 2005 *J. Phys. D: Appl. Phys.* **38** 1690
[42] Belostotskiy S G, Khandelwal R, Wang Q, Donnelly V M, Economou D J and Sadeghi N 2008 *Appl. Phys. Lett.* **92** 221507
[43] Wagenaars E, Gans T, O'Connell D and Niemi K 2012 *Plasma Sources Sci. Technol.* **21** 042002
[44] Wang Q, Doll F, Donnelly V M, Economou D J, Sadeghi N and Franz G F 2007 *J. Phys. D: Appl. Phys.* **40** 4202
[45] Winter J *et al* 2011 Understanding microplasmas arXiv:1104.5385
[46] Niermann B, Hemke T, Babaeva N Y, Boke M, Kushner M J, Mussenbrock T and Winter J 2011 *J. Phys. D: Appl. Phys.* **44** 485204
[47] Dogariu A, Shneider M N and Miles R B 2013 Versatile Radar measurement of the electron loss rate in air *Appl. Phys. Lett.* **103** 224102
[48] Dogariu A, Shneider M N and Miles R 2011 Measurement of electron loss rates in atmospheric pressure air by Radar REMPI *AIAA 2011-1324, 49th AIAA Aerospace Sciences* (*Orlando, FL, 4–7 January 2011*)
[49] Zhang Z, Shneider M N and Miles R B 2007 *Phys. Rev. Lett.* **98** 265005
[50] Shneider M N and Miles R B 2005 *J. Appl. Phys.* **98** 033301
[51] Zhang Z, Shneider M N and Miles R B 2006 *J. Appl. Phys.* **100** 074912
[52] Shashurin A, Shneider M N, Dogariu A, Miles R B and Keidar M 2009 *Appl. Phys. Lett.* **94** 231504
[53] Shashurin A, Shneider M N and Keidar M 2012 *Plasma Sources Sci. Technol.* **21** 034006 and *Erratum* 2012 **21** 049601
[54] Šimek M 2014 Optical diagnostics of streamer discharges in atmospheric gases *J. Phys. D: Appl. Phys.* **47** 463001
[55] Kim Y H, Hong Y J, Baik K Y, Kwon G C, Choi J J, Cho G S, Uhm H S, Kim D Y and Choi E H 2014 Measurement of reactive hydroxyl radical species inside the biosolutions during non-thermal atmospheric pressure plasma jet bombardment onto the solution *Plasma Chem. Plasma Process.* **34** 457–72
[56] Schmidt-Bleker A, Winter J, Iseni S, Dünnbier M, Weltmann K-D and Reuter S 2014 Reactive species output of a plasma jet with a shielding gas device—combination of FTIR absorption spectroscopy and gas phase modeling *J. Phys. D: Appl. Phys.* **47** 145201
[57] Van Ham B T J, Hofmann S, Brandenburg R and Bruggeman P J 2014 *In situ* absolute air, O_3 and NO densities in the effluent of a cold RF argon atmospheric pressure plasma jet obtained by molecular beam mass spectrometry *J. Phys. D: Appl. Phys.* **47** 224013
[58] Pipa A V *et al* 2008 *J. Phys. D: Appl. Phys.* **41** 7
[59] Van Gessel A F H, Hrycak B, Jasinski M, Mizeraczyk J, Van der Mullen J J A M and Bruggeman P J 2013 Temperature and NO density measurements by LIF and OES on an atmospheric pressure plasma jet *J. Phys. D: Appl. Phys.* **46** 095201
[60] Dawson G A and Winn W P 1965 A model for streamer propagation *Z. Phys.* **183** 159–71
[61] Gallimberti I 1972 A computer model for streamer propagation *J. Phys. D: Appl. Phys.* **5** 2179
[62] Lu X, Naidis G V, Laroussi M and Ostrikov K 2014 Guided ionization waves: theory and experiments *Phys. Rep.* **540** 123–66
[63] Naidis G V 2011 *J. Phys. D: Appl. Phys.* **44** 215203
[64] Naidis G V 2012 *J. Appl. Phys.* **112** 103304
[65] Sakiyama Y, Graves D B, Jarrige J and Laroussi M 2010 *Appl. Phys. Lett.* **96** 041501
[66] Van Gaens W and Bogaerts A 2013 *J. Phys. D: Appl. Phys.* **46** 275201
[67] Babaeva N Yu and Kushner M J 2013 *J. Phys. D: Appl. Phys.* **46** 025401
[68] Babaeva N Yu, Ning N, Graves D B and Kushner M J 2012 *J. Phys. D: Appl. Phys.* **45** 115203
[69] Babaeva N Yu and Kushner M J 2013 *J. Phys. D: Appl. Phys.* **46** 125201
[70] Sakiyama Y, Graves D B, Chang H W, Shimizu T and Morfill G E 2012 *J. Phys. D: Appl. Phys.* **45** 425201
[71] Takai E *et al* 2014 *J. Phys. D: Appl. Phys.* **47** 285403
[72] Lukes P, Dolezalova E, Sisrova I and Clupek M 2014 *Plasma Sources Sci. Technol.* **23** 015019
[73] Ratovitski E A, Cheng X, Yan D, Sherman J H, Canady J, Trink B and Keidar M 2014 Anti-cancer therapies of 21-st century. Novel approach to treat human cancers using cold atmospheric plasma *Plasma Process. Polym.* **11** 1128–37
[74] Stoffels E, Flikweert A J, Stoffels W W and Kroesen G M W 2002 Plasma needle: a non-destractive atmospheric plasma source for fine surface treatment of (bio)materials *Plasma Sources Sci. Technol.* **11** 383
[75] Stoffels E, Sakiyama Y and Graves D 2008 Cold atmospheric plasma: charged species and their interaction with cells and tissues *IEEE Trans. Plasma Sci.* **36** 1441–57
[76] Weltmann K-D, Polak M, Masur K, Woedtke T V, Winter J and Reuter S 2012 Plasma processes and plasma sources in medicine *Contrib. Plasma Phys.* **52** 644–54
[77] Hynes R O 2002 Integrins: bidirectional, allosteric signaling machines *Cell* **110** 673
[78] Shashurin A, Stepp M A, Hawley T S, Pal-Ghosh S, Brieda L, Bronnikov S, Jurjus R A and Keidar M 2010 Influence of cold atmospheric jet on surface integrin expression of living cells *Plasma Process. Polym.* **7** 294–300
[79] Regent M *et al* 2011 *Eur. J. Cell Biol.* **90** 261
[80] Georgescu N and Lupu A R 2010 Tumoral and normal cells treatment with high-voltage pulsed cold atmospheric plasma jets *IEEE Trans. Plasma Sci.* **38** 1
[81] Zirnheld J L, Zucker S N, DiSanto T M, Berezney R and Etemadi K 2010 Nonthermal plasma needle: development and targeting of melanoma cells *IEEE Trans. Plasma Sci.* **38** 948
[82] Kim G-C, Lee H J and Shon C-H 2009 The effects of micro plasma on melanoma (G361) cancer cells *J. Korean Phys. Soc.* **54** 625–32
[83] Fridman G, Shereshevsky A, Jost M M, Brooks A D, Fridman A, Gutsol A, Vasilets V and Friedman G 2007 *Plasma Chem. Plasma Process.* **27** 163
[84] Vandamme M, Robert E, Pesnel S, Barbosa E, Dozias S, Sobilo J, Lerondel S, Le Pape A and Pouvesle J M 2010 Antitumor effect of plasma treatment on U87 glioma xenografts: preliminary results *Plasma Process. Polym.* **7** 264

[85] Haertel B *et al* 2012 Surface molecules on HaCaT keratinocytes after interaction with non-thermal atmospheric pressure plasma *Cell Biol. Int.* **36** 1217–22

[86] Wang M, Holmes B, Cheng X, Zhu W, Keidar M and Zhang L 2013 Cold atmospheric plasma for selectively ablating metastatic breast cancer *PloS One* **8** e73741

[87] Guerrero-Preston R, Ogawa T, Uemura M, Shumulinsky G, Valle B, Pirini F, Ravi R, Sidransky D, Keidar M and Trink B 2014 Cold atmospheric plasma treatment selectively targets head and neck squamous cell carcinoma cells *Int. J. Mol. Med.* **34** 941–6

[88] Fridman G, Shereshevsky A, Jost M, Brooks A, Fridman A, Gutsol A, Vasilets V and Friedman G 2007 *Plasma Chem. Plasma Process*. **27** 163

[89] Walk R M, Snyder J A, Srinivasan P, Kirsch J, Diaz S O, Blanco F C, Shashurin A, Keidar M and Sandler A D 2013 Cold atmospheric plasma for the ablative treatment of neuroblastoma *J. Pediatr. Surg.* **48** 67–73

[90] Tanaka H, Mizuno M, Ishikawa K, Nakamura K, Kajiyama H, Kano H, Kikkawa F and Hori M 2011 Plasma-activated medium selectively kills glioblastoma brain tumor cells by down-regulating a survival signaling molecule, AKT kinase *Plasma Med.* **1** 265–77

[91] Yan D, Sherman J H, Cheng X, Ratovitski E, Canady J and Keidar M 2014 *Appl. Phys. Lett.* **105** 224101

[92] Kaushik N K, Kim Y H, Han Y G and Choi E H 2013 Effect of jet plasma on T98G human brain cancer cells *Curr. Appl. Phys.* **13** 176–80

[93] Trink B, Keidar M, Canady J, Abelson S, Shamai Y, Berger L, Skorecki K and Tzukerman M 2014 The effect of cold plasma treatment on cancer stem cells *5th Int. Conf. on Plasma Medicine* (*Nara, Japan, May 18–22 2014*)

[94] Schlegel J, Koritzer J and Boxhammer V 2013 *Clin. Plasma Med*. **1** 2

[95] Brulle L *et al* 2012 Effects of a non thermal plasma treatment alone or in combination with gemcitabine in a MIA $PaCa_2$-luc orthotopic pancreatic carcinoma model *PLoS One* **7** e52653

[96] Koritzer J *et al* 2013 Restoration of sensitivity in chemo-resistant glioma cells by cold atmospheric plasma *PLoS One* **8** e64498

[97] Snyder J A, Srinivasan P, Walk R M, Shashurin A, Keidar M and Sandler A D 2012 *Cold Atmospheric Plasma Induces Neuroblastoma Ablation via Reactive Oxygen Species Production, presented at American Academy of Pediatrics (AAP) National Conference and Exhibition* (*New Orleans, LA, October 20–23 2012*)

[98] Szili E J *et al* 2014 A 'tissue model' to study the plasma delivery of reactive oxygen species *J. Phys. D: Appl. Phys*. **47** 152002

[99] Collet G *et al* 2014 Plasma jet-induced tissue oxygenation: potentialities for new therapeutic strategies *Plasma Sources Sci. Technol*. **23** 012005

[100] Lord C J and Ashworth A 2012 The DNA damage response and cancer therapy *Nature* **481** 287–94

[101] Connell P P and Hellman S 2009 Advances in radiotherapy and implications for the next century: a historical perspective *Cancer Res.* **69** 383–92

[102] Tsuruo T *et al* 2003 Molecular targeting therapy of cancer: drug resistance, apoptosis and survival signal *Cancer Sci.* **94** 15–21

[103] Schwartz G K and Shah M A 2005 Targeting the cell cycle: a new approach to cancer therapy *J. Clin. Oncol.* **23** 9408–21

[104] Longo D L and Longo D 2010 *Harrison's Hematology and Oncology* (New York: McGraw-Hill Medical) pp 294–318

[105] Bonner W M, Redon C E, Dickey J S, Nakamura A J, Sedelnikova O A, Solier S and Pommier Y 2008 GammaH2AX and cancer *Nat. Rev. Cancer* **8** 957–67

[106] Marti T M, Hefner E, Feeney L, Natale V and Cleaver J E 2006 H2AX phosphorylation within the G1 phase after UV irradiation depends on nucleotide excision repair and not DNA double-strand breaks *Proc. Natl. Acad. Sci.* **103** 9891–6

[107] Zhao H, Dobrucki J, Rybak P, Traganos F, Halicka H D and Darzynkiewicz Z 2011 Induction of DNA damage signaling by oxidative stress in relation to DNA replication as detected using 'click chemistry' *Cytometry* A **79A** 897–902

[108] Graves D 2012 *J. Phys. D: Appl. Phys*. **45** 263001

[109] Watson J 2013 Perspective: oxidants, antioxidants and the current incurability of metastatic cancers *Open Biol*. **3**120144

[110] Cairns R, Harris I and Mak T W 2011 Regulation of cancer cell metabolism *Nat. Rev. Cancer* **11** 85–95

[111] Graves D P 2014 Reactive species from cold atmospheric plasma: implications for cancer therapy *Plasma Process. Polym*. **11** 1120–7

[112] Ahn H, Kim K, Hoan N, Kim C, Moon E, Choi K, Yang S and Lee J 2014 *PLoS One* **9** e86173

[113] Trachootham D, Alexandre J and Huang P 2009 *Nat. Rev. Drug Discovery* **8** 579–91

[114] Ishaq M, Evans M and Ostrikov K 2014 *Int. J. Cancer* **134** 1517–28

[115] Ishaq M, Kumar S, Varinli H, Han Z, Rider A, Evans M, Murphy A and Ostrikov K 2014 *Mol. Biol. Cell*

[116] Fransen M, Nordgren M, Wang B and Apanasets O 2012 Role of peroxisomes in ROS/RNS-metabolism: implications for human disease *Biochim. Biophys. Acta* **1822** 1363–73

[117] Jo S *et al* 2001 *J. Biol. Chem.* **276** 16168–76

[118] Moncada S and Erusalimsky J 2002 *Nat. Rev. Mol. Cell Biol*. **3** 214–20

[119] Szabo C, Ischiropoulos H and Radi R 2007 *Nat. Rev. Drug Discovery* **6** 662–80

[120] Kaushik N K, Kaushik N, Park D and Choi E H 2014 Altered antioxidant system stimulates dielectric barrier discharge plasma-induced cell death for solid tumor cell treatment *PLoS One* **9** e103349

[121] Kalghatgi S *et al* 2011 Effects of nonthermal plasma on mammalian cells *PLoS One* **6** e16270

[122] Cheng X, Sherman J, Murphy W, Ratovitski E, Canady J and Keidar M 2014 *PLoS One* **9** e98652

[123] Ma Y, Ha C, Hwang S, Lee H, Kim G, Lee K and Song K 2014 *PLoS One* **9** e91947

[124] Halperin E C, Perez C A and Brady L W (ed) 2008 *Principles and Practice of Radiation Oncology* 5th edn (Philadelphia, PA: Lippincott, Williams and Wilkins)

[125] Kong M G, Keidar M and Ostrikov K 2011 Plasmas meet nanoparticles—where synergies can advance the frontier of medicine *J. Phys. D: Appl. Phys*. **44** 174018

[126] Kim G C, Kim G J, Park S R, Jeon S M, Seo H J, Iza F and Lee J K 2009 Air plasma coupled with antibody-conjugated nanoparticles: a new weapon against cancer *J. Phys. D. Appl. Phys*. **42** 032005

[127] Cheng X, Murphy W, Recek N, Yan D, Cvelbar U, Vesel A, Mozetic M, Canady J, Keidar M and Sherman J 2014 Synergistic effect of gold nanoparticles and cold plasma on glioblastoma cancer therapy *J. Phys. D: Appl. Phys.* **47** 335402

[128] Enderling H and Rejniak K A 2013 Simulating cancer: computational models in oncology *Front. Oncol*. **3** 233

[129] Keidar M 2014 Towards understanding mechanism of cold atmospheric plasma in cancer treatment *5th Int. Conf. on Plasma Medicine* (*Nara, Japan, 21 May*) (Plenary Talk)

[130] Murphy W, Carroll C and Keidar M 2014 Simulation of the effect of plasma species on tumor growth and apoptosis *J. Phys. D: Appl. Phys.* **47** 472001

[131] Recek N, Cheng X, Keidar M, Cvelbar U, Vesel A, Mozetič M and Sherman J H 2015 Effects of cold plasma on glial cell morphology studied by atomic force microscopy *PLoS One* **10** e0119111